

Undermodeling affects minimal model indexes: insights from a two-compartment model

Andrea Caumo, Paolo Vicini, Jeffrey J. Zachwieja, Angelo Avogaro, Kevin Yarasheski, Dennis M. Bier and Claudio Cobelli
Am J Physiol Endocrinol Metab 276:E1171-E1193, 1999.

You might find this additional info useful...

This article cites 35 articles, 25 of which can be accessed free at:

<http://ajpendo.physiology.org/content/276/6/E1171.full.html#ref-list-1>

This article has been cited by 15 other HighWire hosted articles, the first 5 are:

IVGTT glucose minimal model covariate selection by nonlinear mixed-effects approach

Paolo Denti, Alessandra Bertoldo, Paolo Vicini and Claudio Cobelli

Am J Physiol Endocrinol Metab, May, 2010; 298 (5): E950-E960.

[\[Abstract\]](#) [\[Full Text\]](#) [\[PDF\]](#)

Use of labeled oral minimal model to measure hepatic insulin sensitivity

Chiara Dalla Man, Gianna Toffolo, Rita Basu, Robert A. Rizza and Claudio Cobelli

Am J Physiol Endocrinol Metab, November 1, 2008; 295 (5): E1152-E1159.

[\[Abstract\]](#) [\[Full Text\]](#) [\[PDF\]](#)

Current approaches for assessing insulin sensitivity and resistance in vivo: advantages, limitations, and appropriate usage

Ranganath Muniyappa, Sihoon Lee, Hui Chen and Michael J. Quon

Am J Physiol Endocrinol Metab, January 1, 2008; 294 (1): E15-E26.

[\[Abstract\]](#) [\[Full Text\]](#) [\[PDF\]](#)

Insulin sensitivity by oral glucose minimal models: validation against clamp

Chiara Dalla Man, Kevin E. Yarasheski, Andrea Caumo, Heather Robertson, Gianna Toffolo,

Kenneth S. Polonsky and Claudio Cobelli

Am J Physiol Endocrinol Metab, December 1, 2005; 289 (6): E954-E959.

[\[Abstract\]](#) [\[Full Text\]](#) [\[PDF\]](#)

Measurement of selective effect of insulin on glucose disposal from labeled glucose oral test minimal model

Chiara Dalla Man, Andrea Caumo, Rita Basu, Robert Rizza, Gianna Toffolo and Claudio Cobelli

Am J Physiol Endocrinol Metab, November 1, 2005; 289 (5): E909-E914.

[\[Abstract\]](#) [\[Full Text\]](#) [\[PDF\]](#)

Updated information and services including high resolution figures, can be found at:

<http://ajpendo.physiology.org/content/276/6/E1171.full.html>

Additional material and information about *AJP - Endocrinology and Metabolism* can be found at:

<http://www.the-aps.org/publications/ajpendo>

This information is current as of October 13, 2011.

Undermodeling affects minimal model indexes: insights from a two-compartment model

ANDREA CAUMO,¹ PAOLO VICINI,² JEFFREY J. ZACHWIEJA,³ ANGELO AVOGARRO,⁴ KEVIN YARASHESKI,⁵ DENNIS M. BIER,⁶ AND CLAUDIO COBELLI⁷

¹San Raffaele Scientific Institute, 20100 Milan; ⁴Department of Metabolic Diseases and ⁷Department of Electronics and Informatics, University of Padova, 35131 Padua, Italy;

²Department of Bioengineering, University of Washington, Seattle, Washington 98195;

³Pennington Biomedical Research Center, Louisiana State University, Baton Rouge, Louisiana 70808;

⁵Metabolism Division, Washington University School of Medicine, Saint Louis, Missouri 63110;

and ⁶Children's Nutrition Research Center, Baylor College of Medicine, Houston, Texas 77030-2600

Caumo, Andrea, Paolo Vicini, Jeffrey J. Zachwieja, Angelo Avogaro, Kevin Yarasheski, Dennis M. Bier, and Claudio Cobelli. Undermodeling affects minimal model indexes: insights from a two-compartment model. *Am. J. Physiol.* 276 (*Endocrinol. Metab.* 39): E1171–E1193, 1999.— The classic (hereafter cold) and the labeled (hereafter hot) minimal models are powerful tools to investigate glucose metabolism. The cold model provides, from intravenous glucose tolerance test (IVGTT) data, indexes of glucose effectiveness (S_G) and insulin sensitivity (S_I) that measure the effect of glucose and insulin, respectively, to enhance glucose disappearance and inhibit endogenous glucose production. The hot model provides, from hot IVGTT data, indexes of glucose effectiveness (S_G^*) and insulin sensitivity (S_I^*) that, respectively, measure the effects of glucose and insulin on glucose disappearance only. Recent reports call for a reexamination of some of the assumptions of the minimal models. We have previously pointed out the criticality of the single-compartment description of glucose kinetics on which both the minimal models are founded. In this paper we evaluate the impact of single-compartment undermodeling on S_G , S_I , S_G^* , and S_I^* by using a two-compartment model to describe the glucose system. The relationships of the minimal model indexes to the analogous indexes measured with the glucose clamp technique are also examined. Theoretical analysis and simulation studies indicate that cold indexes are more affected than hot indexes by undermodeling. In particular, care must be exercised in the physiological interpretation of S_G , because this index is a local descriptor of events taking place in the initial portion of the IVGTT. As a consequence, S_G not only reflects glucose effect on glucose uptake and production but also the rapid exchange of glucose between the accessible and nonaccessible glucose pools that occurs in the early part of the test.

insulin sensitivity; glucose effectiveness; mathematical model; intravenous glucose tolerance test; glucose clamp

THE INTRAVENOUS GLUCOSE TOLERANCE TEST (IVGTT), standard or modified with a tolbutamide or insulin injection, interpreted with the classic minimal model of glucose disappearance (hereafter cold minimal model) (6–10), is a powerful research tool to investigate glu-

cose metabolism in physiopathological and epidemiological studies; more than 350 papers have appeared until 1998. The model provides two metabolic indexes measuring glucose effectiveness (S_G) and insulin sensitivity (S_I). S_G and S_I are composite parameters, i.e., they measure the overall effect of glucose and insulin, respectively, to enhance glucose disappearance (R_d) and inhibit endogenous glucose production (EGP). To segregate the effect of glucose and insulin on R_d and EGP, a labeled (hereafter hot) IVGTT has been introduced, i.e., a glucose tracer has been added to the glucose bolus (2, 17, 19, 23). The hot IVGTT interpreted with a minimal model of labeled glucose disappearance (hereafter hot minimal model) provides new indexes of glucose effectiveness (S_G^*) and insulin sensitivity (S_I^*) that measure the effects of glucose and insulin, respectively, on glucose disposal only (19, 23).

Several investigators have recently reexamined some of the minimal model assumptions (16–18, 22–24, 27, 30, 32). We have found some unexpected relationships between the cold and hot indexes (17, 19); in addition, we have observed that when EGP is derived by combining the cold and hot minimal models, its time course is physiologically absurd (17). Quon et al. (30) have shown in a study on insulin-dependent diabetes mellitus patients that S_G is likely to be overestimated. Saad et al. (32) have shown that S_I obtained from an insulin-modified IVGTT is well correlated but markedly underestimated compared with the insulin sensitivity index obtained with the glucose clamp technique. Finegood and Tzur (24) have shown in dogs that decreased S_G associated with decreased insulin response is an artifact of the minimal model method and that S_G is poorly correlated with the glucose effectiveness index obtained with the glucose clamp technique.

We have suggested two possible areas of model error (16, 18, 22, 23, 38): the monocompartmental structure of both the minimal models and the description of EGP embodied in the cold minimal model. We have shown that the monocompartmental structure is the major area responsible for the implausible EGP profile and

that a two-compartment hot minimal model provides not only a reliable profile of EGP by deconvolution (14, 39) but also tracer-based indexes of glucose effectiveness, insulin sensitivity, and plasma clearance rate (37). Recently, we have used the two-compartment paradigm (18, 22, 38) to explain the findings of Quon et al. (30) and Saad et al. (32) and the poor agreement between S_G and the clamp-based index of glucose effectiveness (24).

The aim of the present paper is to use a two-compartment model of glucose metabolism to explain the mechanisms by which monocompartmental under-modeling affects both cold and hot minimal model indexes.

Glossary

$A_1, A_2; A_1^*, A_2^*$	Coefficients of two-exponential cold and hot glucose decay during an IVGTT at basal insulin, mg/dl and dpm/ml (for a radiolabeled IVGTT)
D, D^*	Cold and hot glucose IVGTT dose, mg/kg and dpm/kg, respectively
$EGP(t)$	Endogenous glucose production, $mg \cdot kg^{-1} \cdot min^{-1}$
EGP_b	Endogenous glucose production in the basal state, $mg \cdot kg^{-1} \cdot min^{-1}$
$g(t), g^*(t)$	Cold and hot glucose concentration in plasma, mg/dl and dpm/ml, respectively
$g(0), g^*(0)$	Minimal model estimates of cold and hot glucose concentration at <i>time 0</i> ⁺ , mg/dl and dpm/ml, respectively
g_b	Plasma glucose concentration in basal state, mg/dl
$g_2(t), \tilde{g}_2^*(t)$	Cold and hot glucose concentration in the second pool of the two-compartment model, mg/dl and dpm/ml, respectively
$\tilde{g}_2(t), \tilde{g}_2^*(t)$	As above, with insulin-dependent removal moved to the accessible pool, mg/dl and dpm/ml, respectively
GE, GE^*	Cold and hot glucose effectiveness of the two-compartment model, $ml \cdot kg^{-1} \cdot min^{-1}$
GE_b	Cold glucose effectiveness measured from the area under the glucose excursion during an IVGTT at basal insulin, $ml \cdot kg^{-1} \cdot min^{-1}$
$GINF(t)$	Glucose infusion rate during the glucose clamp, $mg \cdot kg^{-1} \cdot min^{-1}$
$k_{21}, k_{12}, k_{02}, k_d$	Rate parameters of the two-compartment model, min^{-1}
k_{22}	$k_{22} = k_{12} + k_{02}$, min^{-1}
k_a	Rate constant of the remote insulin compartment in the two-compartment model, min^{-1}
k_{bd}, k_{bp}	Parameters describing insulin effect on glucose uptake and EGP in the two-compartment model, $min^{-2} \cdot ml \cdot \mu U^{-1}$, respectively
k_p	Parameter describing glucose effect on EGP in the two-compartment model, min^{-1}

$i(t)$	Insulin concentration in plasma, $\mu U/ml$
i_b	Plasma insulin concentration in the basal state, $\mu U/ml$
IS, IS^*	Cold and hot insulin sensitivity of the two-compartment model, $ml \cdot kg^{-1} \cdot min^{-1}$ per $\mu U/ml$
PCR_b	Plasma glucose clearance in the basal state, $ml \cdot kg^{-1} \cdot min^{-1}$
$p_1, p_2; p_1^*, p_2^*$	Cold and hot minimal model rate parameters, min^{-1}
$q_i(t), q_i^*(t)$	Cold and hot glucose mass in <i>i</i> th compartment of the two-compartment model (<i>i</i> = 1, 2), mg and dpm, respectively
$R_d(t)$	Glucose disappearance rate from the accessible pool, $mg \cdot kg^{-1} \cdot min^{-1}$
$R_{d,0}$	Nonzero intercept of the relationship R_d vs. g , $mg \cdot kg^{-1} \cdot min^{-1}$
S_G, S_G^*	Minimal model estimates of cold and hot glucose effectiveness, min^{-1}
$S_{G(\text{clamp})}, S_{G,d(\text{clamp})}$	Glucose clamp measurements of cold and hot glucose effectiveness, $ml \cdot kg^{-1} \cdot min^{-1}$
S_I, S_I^*	Minimal model estimates of cold and hot insulin sensitivity, $min^{-1} \cdot \mu U \cdot ml^{-1}$
$S_{I(\text{clamp})}, S_{I,d(\text{clamp})}$	Glucose clamp measurements of cold and hot insulin sensitivity, $ml \cdot kg^{-1} \cdot min^{-1} \cdot \mu U^{-1} \cdot ml$
t	Time, min
V, V^*	Cold and hot minimal model volume, ml/kg
V_1	Volume of the accessible pool of the two-compartment model, ml/kg
V_T	Total glucose distribution volume, ml/kg
$x(t), x^*(t)$	Cold and hot minimal model insulin action, min^{-1}
$X(t)$	Two-compartment model insulin action, i.e., $X = x_p + x_d$, min^{-1}
$\tilde{X}(t)$	As above, with insulin-dependent removal moved to the accessible pool, i.e., $\tilde{X} = x_p + \tilde{x}_d$, min^{-1}
$x_d(t)$	Two-compartment model insulin action on glucose uptake, min^{-1}
$\tilde{x}_d(t), \tilde{x}_d^*(t)$	As above, with insulin-dependent removal moved to the accessible pool (the asterisk denotes tracer-based calculation), min^{-1}
$x_p(t)$	Two-compartment model insulin action on EGP, min^{-1}
$\alpha(t)$	Deviation of hot glucose decay from a two-exponential function during an IVGTT at basal insulin, dpm/ml
γ	$\gamma = k_{21}k_{12}$, min^{-2}
$\lambda_1, \lambda_2; \lambda_1^*, \lambda_2^*$	Fast and slow eigenvalues of the cold and hot glucose decay during an IVGTT at basal insulin, min^{-1}

THE COLD AND HOT MINIMAL MODELS

The Cold Model

The cold minimal model (Fig. 1) interprets plasma glucose and insulin concentrations measured during an IVGTT (standard, or modified with a tolbutamide or

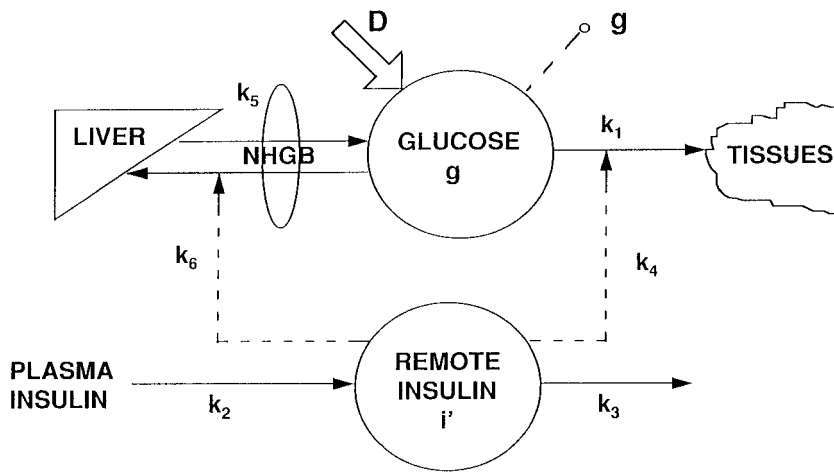


Fig. 1. The cold minimal model. See glossary for definition of terms.

insulin injection). The model in its uniquely identifiable parametrization (6, 8, 9, 23) is described by

$$\begin{aligned} \dot{g}(t) &= -[p_1 + x(t)]g(t) + p_1g_b & g(0) &= g_b + \frac{D}{V} \\ \dot{x}(t) &= -p_2x(t) + p_3[i(t) - i_b] & x(0) &= 0 \end{aligned} \quad (1)$$

where g is plasma glucose concentration (g_b denotes its basal end test value), i is plasma insulin concentration (i_b denotes its basal end test value), D is the glucose dose in the bolus, V is the glucose distribution volume, x is insulin action [$x = (k_4 + k_6)i'$, where i' is insulin in the remote compartment], and the p_i values are parameters related to the k_i values: $p_1 = k_1 + k_5$, $p_2 = k_3$, $p_3 = k_2(k_4 + k_6)$.

Parameters p_1 , p_2 , p_3 , and V can be estimated from glucose and insulin data by use of nonlinear least squares parameter estimation techniques (13). From them one can calculate the cold indexes of glucose effectiveness, S_G , and insulin sensitivity, S_I , as

$$\begin{aligned} S_G &= p_1 = k_1 + k_5 \quad (\text{min}^{-1}) \\ S_I &= \frac{p_3}{p_2} = \frac{k_2(k_4 + k_6)}{k_3} \quad (\text{min}^{-1} \cdot \mu\text{U}^{-1} \cdot \text{ml}) \end{aligned} \quad (2)$$

S_G and S_I measure the effects of glucose and insulin, respectively, on both R_d and EGP. In fact, because S_G is a function not only of k_1 , but also of k_5 (see Fig. 1), it measures the ability of glucose at basal insulin to stimulate R_d and to inhibit EGP. Similarly, S_I is a function not only of k_1 , k_3 , k_4 , but also of k_6 , and thus measures the ability of insulin to enhance the glucose stimulation of R_d and inhibition of EGP. Parameter p_2 is the rate constant of the remote insulin compartment and governs the speed of rise and decay of insulin action.

Reference values for S_G and S_I have been obtained from the analysis of insulin and cold glucose data of a hot IVGTT performed in 25 normal young adults. Values for S_G and S_I were, respectively, $0.026 \pm 0.002 \text{ min}^{-1}$ and $7.3 \pm 1.0 \times 10^{-4} \text{ min}^{-1} \cdot \mu\text{U}^{-1} \cdot \text{ml}$. The mean

precision of S_G and S_I estimates was 49 and 18%, respectively. Volume V was estimated as $1.66 \pm 0.05 \text{ dl/kg}$.

The Hot Model

The hot minimal model (Fig. 2) interprets plasma hot glucose and insulin concentrations measured during a hot IVGTT, that is, an IVGTT (standard, or modified with a tolbutamide or insulin injection) in which a glucose tracer (radioactive or stable isotope) is added to the glucose bolus. Because hot glucose concentration only reflects R_d , the hot model yields indexes measuring glucose and insulin effect on R_d only. The model in its uniquely identifiable parametrization (2, 17, 19, 23) is described by

$$\begin{aligned} \dot{g}^*(t) &= -[p_1^* + x^*(t)]g^*(t) & g^*(0) &= \frac{D^*}{V^*} \\ \dot{x}^*(t) &= -p_2^*x^*(t) + p_3^*[i(t) - i_b] & x^*(0) &= 0 \end{aligned} \quad (3)$$

where the symbols are the same as in Eq. 1, with the asterisk denoting tracer-related variables and parameters. In particular, D^* is the hot glucose dose, V^* is the hot glucose distribution volume, x^* is hot insulin action

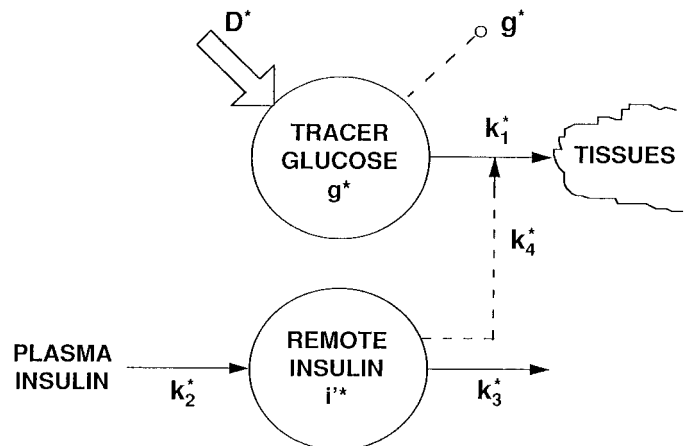


Fig. 2. The hot minimal model. See glossary for definition of terms.

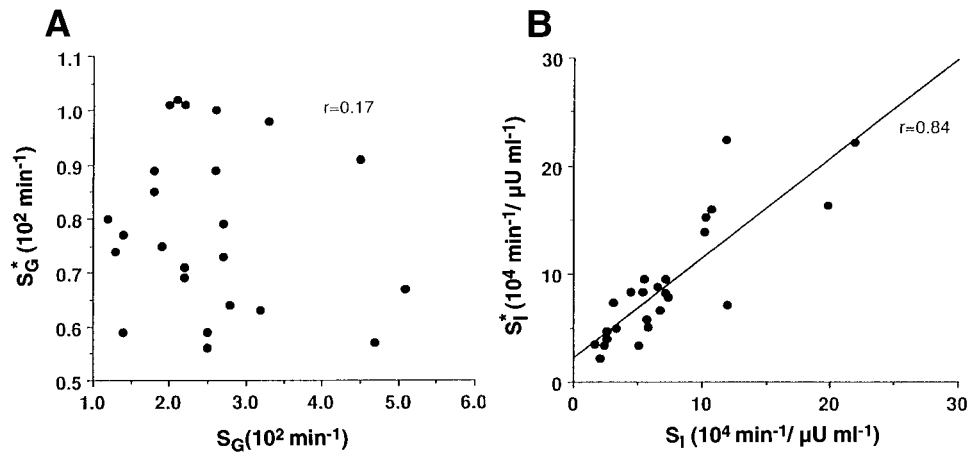


Fig. 3. Correlation between cold and hot indexes of glucose effectiveness (A) and insulin sensitivity (B). See glossary for definition of terms.

(proportional to remote insulin i'^* , $x^* = k_4 i'^*$), and the p_i^* values are parameters related to the k_i values: $p_1^* = k_1$, $p_2^* = k_3$, and $p_3^* = k_2 k_4$.

Parameters p_1^* , p_2^* , p_3^* , and V^* can be estimated from insulin and hot glucose data by using nonlinear least squares parameter estimation techniques (13). From them one can calculate the hot indexes of glucose effectiveness, S_G^* , and insulin sensitivity, S_I^* , as

$$S_G^* = p_1^* = k_1 \quad (\text{min}^{-1})$$

$$S_I^* = \frac{p_3^*}{p_2^*} = \frac{k_2 k_4}{k_3} \quad (\text{min}^{-1} \cdot \mu\text{U}^{-1} \cdot \text{ml}) \quad (4)$$

S_G^* measures the ability of glucose at basal insulin to stimulate R_d , and S_I^* measures the ability of insulin to enhance glucose stimulation of R_d . Parameter p_2^* is the rate constant of the remote insulin compartment and governs the speed of rise and decay of hot insulin action.

Values for S_G^* and S_I^* have been obtained in the same 25 normal young subjects from the analysis of insulin and hot glucose data of the hot IVGTT. Data on 15 subjects have already been reported in previous publications (2, 17). Stable isotopes ($[6\text{-}^2\text{H}_2]\text{glucose}$ and $[2\text{-}^2\text{H}]\text{glucose}$) were employed in 19 studies, whereas a radioactive isotope ($[3\text{-}^3\text{H}]\text{glucose}$) was employed in 6 studies. Values for S_G^* and S_I^* were, respectively, $0.0082 \pm 0.0003 \text{ min}^{-1}$ and $9.0 \pm 1.2 \times 10^{-4} \text{ min}^{-1} \cdot \mu\text{U}^{-1} \cdot \text{ml}$. The mean precision of S_G^* and S_I^* estimates was 4 and 5%, respectively. Volume V^* was estimated as $1.88 \pm 0.06 \text{ dl/kg}$.

Cold vs. Hot Indexes

The results of this study confirm previously observed trends (2, 17, 19): S_G is about three times higher than S_G^* ($P < 0.001$), and S_I is lower than S_I^* ($P < 0.05$). Of note is that these trends are also present when the indexes are estimated from an insulin-modified hot IVGTT (unpublished results). Thanks to the larger data base, it is now possible to assess the degree of correlation between S_G and S_G^* and between S_I and S_I^*

(Fig. 3). Whereas a strong correlation exists between S_I and S_I^* ($r = 0.84$, $P < 0.001$), S_G and S_G^* are uncorrelated ($r = 0.17$, $P > 0.15$).

Some of the above results are unexpected and suggest the presence of some model error. S_G is higher than S_G^* , in keeping with the theoretical expectation, but their ratio is too high compared with that of the analogous clamp-based indexes of cold, $S_{G(\text{clamp})}$, and hot, $S_{G,d(\text{clamp})}$, glucose effectiveness (subscript "d" denotes disappearance). In fact, whereas S_G is about three times higher than S_G^* , $S_{G(\text{clamp})}$ is only 1.5 times higher than $S_{G,d(\text{clamp})}$ (11). Also, the complete lack of correlation between S_G and S_G^* is surprising, because $S_{G(\text{clamp})}$ and $S_{G,d(\text{clamp})}$ are presumably well correlated, given that $S_{G,d(\text{clamp})}$ is the major determinant ($\sim 2/3$) of $S_{G(\text{clamp})}$ (11).

The time courses of cold and hot insulin actions (Fig. 4) also show an unexpected trend. The cold minimal model assumes that insulin actions on R_d and EGP have the same timing, but the time lag between x and x^* (caused by p_2 being lower than p_2^*) violates this assumption. In addition, the profile of insulin action on EGP, calculated as the difference $x - x^*$, is physiologically implausible (17).

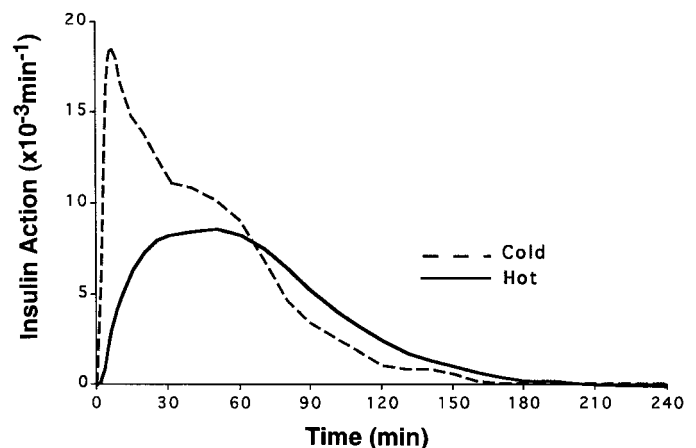


Fig. 4. Cold and hot insulin action during a standard hot intravenous glucose tolerance test (IVGTT) in a representative subject.

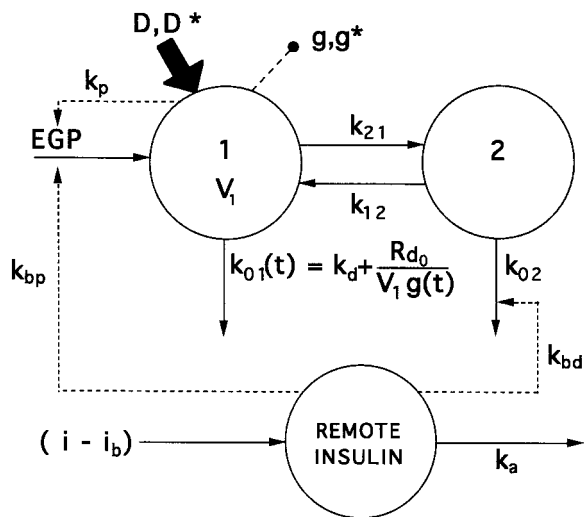


Fig. 5. The two-compartment simulation model. See glossary for definitions of terms.

Finally, the finding $S_I < S_I^*$ is unexpected, because S_I , which measures insulin effect on both R_d and EGP, should be higher than S_I^* , which measures insulin effect on R_d only. This incongruity is not present when insulin sensitivity is assessed with the glucose clamp technique: in Ref. 10 $S_{I(\text{clamp})}$ exceeded $S_{I,d(\text{clamp})}$ [denoted as $S_{I,p(\text{clamp})}$ in that paper] in each subject, with $S_{I(\text{clamp})}$ and $S_{I,d(\text{clamp})}$ being the clamp version analogous to S_I and S_I^* , respectively.

The above inconsistencies are symptoms of model error. Two possible areas of error are the description of glucose and insulin effect on EGP embodied in the cold model and the single-compartment description of glucose kinetics (17, 18, 23). In this paper we focus on the latter only.

A TWO-COMPARTMENT MODEL OF THE GLUCOSE SYSTEM DURING THE IVGTT

To investigate the mechanisms by which single-compartment undermodeling affects the minimal model indexes, we developed a physiologically based two-compartment model to describe the glucose system during the IVGTT. The model, shown in Fig. 5, is described in detail in APPENDIX A. Briefly, the model describes both glucose kinetics and EGP during the IVGTT. The description of glucose kinetics is the same as that of the two-compartment minimal model proposed in Refs. 14 and 37. It is assumed that insulin-independent glucose disposal occurs in the accessible compartment, whereas insulin-dependent glucose disposal occurs in the nonaccessible compartment. Consistent with known physiology, insulin-independent glucose uptake accounts for the inhibitory effect of hyperglycemia on glucose clearance. It consists of two components, one constant and the other proportional to glucose concentration. Insulin-dependent glucose uptake is parametrically controlled by insulin in a remote insulin compartment. The assumption is made that, in the basal state, insulin-dependent glucose disposal is

three times insulin-independent glucose disposal. EGP is described using the same functional description embodied in the cold minimal model (8, 17, 19, 23), thus allowing us to focus on the bias due to single-compartment undermodeling only. In fact, EGP inhibition is assumed to be proportional to the increment of glucose concentration above basal and to the product of glucose concentration and insulin action. In addition, as in the minimal model, insulin action on EGP is assumed to have the same timing as insulin action on glucose uptake.

To ascertain the ability of this model to describe satisfactorily the glucose system during the IVGTT, we used Monte Carlo simulation (details in APPENDIX B). Briefly, the two-compartment model with mean parameters was used to generate noise-free cold and hot glucose data during a hot IVGTT. The mean insulin profile of either a standard or an insulin-modified IVGTT was used as input to the model. Noise of appropriate characteristics was added to the data, and the noisy IVGTT data sets were then interpreted with the minimal models. We reasoned that, if the two-compartment model is a realistic representation of the glucose system during the IVGTT, the minimal model parameters estimated from the simulated data should be close to those estimated from real data and should exhibit the same trends discussed above. In addition, the relationships between the minimal model estimates of glucose effectiveness and insulin sensitivity and the analogous two-compartment model indexes should be similar to those observed experimentally between the minimal model and clamp-based indexes. These hypotheses were all confirmed. Table 1 reports the mean results of the identification of the two minimal models from simulated IVGTT data. The values of S_G , S_I , S_G^* , and S_I^* are similar to those reported in the literature. In particular, S_I is close to the value found by Saad et al. (32) in normal subjects. This similarity is noteworthy, because the insulin sensitivity of the two-compartment model has been chosen equal to the one found by Saad et al. in normal subjects with the clamp technique (see APPENDIX A). Of note is that all the experimentally observed inconsistencies between cold

Table 1. Monte Carlo simulation results: cold and hot minimal model indexes estimated from standard and insulin-modified IVGTT

	Cold Minimal Model			Hot Minimal Model		
	S_G , min ⁻¹	S_I , $\times 10^{-4}$ dl· kg ⁻¹ ·min ⁻¹ · μU^{-1} ·ml	V, dl/kg	S_G^* , min ⁻¹	S_I^* , $\times 10^{-4}$ dl· kg ⁻¹ ·min ⁻¹ · μU^{-1} ·ml	V^* , dl/kg
Standard IVGTT	0.021	2.9	2.0	0.0102	3.2	2.1
Insulin-modified IVGTT	0.020	3.3	1.9	0.0098	3.5	2.2

IVGTT, intravenous glucose tolerance test; S_G and S_G^* , cold and hot indexes of glucose effectiveness, respectively; S_I and S_I^* , cold and hot indexes of insulin sensitivity, respectively; V and V^* , cold and hot minimal model volumes, respectively.

and hot parameters are present: S_I is lower than S_I^* , S_G is twice S_G^* , and hot insulin action is faster than cold because $p_2^* > p_2$ (e.g., for the simulated standard IVGTT, $p_2^* = 0.069$ vs. $p_2 = 0.027 \text{ min}^{-1}$).

How do the minimal model indexes of glucose effectiveness and insulin sensitivity compare with the “true” indexes of the two-compartment model? To answer this question we derived indexes of glucose effectiveness, insulin sensitivity, and basal plasma clearance rate for the two-compartment model (details are provided in APPENDIX C). Of note is that these indexes are expressed in the same units as those of the corresponding clamp-based indexes. To express also the minimal model indexes in the same units, S_G and S_I were multiplied by V , and S_G^* and S_I^* were multiplied by V^* , in keeping with the analysis reported in Vicini et al. (37). The values of the two-compartment and minimal model indexes are reported in Table 2. One can see that the cold minimal model overestimates glucose effectiveness and underestimates insulin sensitivity, in keeping with the experimental results (24, 32). $S_G^*V^*$ slightly underestimates basal glucose clearance and markedly overestimates hot glucose effectiveness, in keeping with the trend observed in Ref. 37. Specifically, S_G^* is virtually identical to the basal fractional glucose clearance of the two-compartment model (e.g., S_G^* from the standard IVGTT is 0.0102 min^{-1} , and $\text{PCR}/V_T = 0.0096 \text{ min}^{-1}$). This is consistent with the results of the S_G^* validation study in dogs (19). $S_I^*V^*$ slightly underestimates the hot insulin sensitivity of the two-compartment model, but no studies are available in the literature comparing the hot minimal model insulin sensitivity with the analogous clamp-based index.

All in all, these results support the notion that the two-compartment model is a satisfactory representation of the glucose system during the IVGTT. We can thus use this model with confidence to analyze the impact of monocompartmental undermodeling on the cold and hot minimal model indexes and elucidate their

Table 2. Cold and hot glucose effectiveness and insulin sensitivity and basal plasma clearance rate for 2-compartment model and minimal models during a standard and an insulin-modified IVGTT

	Two-Compartment Model	Minimal Models	
		Standard IVGTT	Insulin-modified IVGTT
Cold glucose effectiveness, $\text{ml} \cdot \text{kg}^{-1} \cdot \text{min}^{-1}$	GE = 2.1	$S_G V = 4.1$	$S_G V = 3.9$
Hot glucose effectiveness, $\text{ml} \cdot \text{kg}^{-1} \cdot \text{min}^{-1}$	GE* = 1.4	$S_G^* V^* = 2.2$	$S_G^* V^* = 2.1$
Cold insulin sensitivity, $\times 10^{-2} \text{ ml} \cdot \text{kg}^{-1} \cdot \text{min}^{-1}$ per $\mu\text{U}/\text{ml}$	IS = 10.2	$S_I V = 5.8$	$S_I V = 6.4$
Hot insulin sensitivity, $\times 10^{-2} \text{ ml} \cdot \text{kg}^{-1} \cdot \text{min}^{-1}$ per $\mu\text{U}/\text{ml}$	IS* = 7.9	$S_I^* V^* = 6.7$	$S_I^* V^* = 7.7$
Basal plasma clearance rate, $\text{ml} \cdot \text{kg}^{-1} \cdot \text{min}^{-1}$	PCR _b = 2.5	$S_G^* V^* = 2.2$	$S_G^* V^* = 2.1$

See glossary for definition of terms.

relationships with the analogous clamp-based measures of glucose effectiveness and insulin sensitivity.

COLD GLUCOSE EFFECTIVENESS

Effects of Monocompartmental Undermodeling on S_G

To examine the effects of the monocompartmental approximation on S_G , we build on Ref. 18 and, for the sake of clarity, we outline the reasoning followed in that paper. Usually, S_G is estimated from an IVGTT in which an insulin response is present and glucose decay depends on both glucose and insulin. However, the effects of the monocompartmental approximation on S_G can be more easily determined if one first analyzes what happens during an IVGTT in which insulin is maintained at the basal level. Under these conditions, insulin action is identically equal to zero (Eq. 1), and the minimal model is described by a first-order linear differential equation

$$\dot{g}(t) = -S_G[g(t) - g_b] \quad g(0) = g_b + \frac{D}{V} \quad (5)$$

Solving Eq. 5 for glucose concentration and defining $\Delta g(t) = g(t) - g_b$, one has

$$\Delta g(t) = \frac{D}{V} e^{-S_G t} \quad (6)$$

Thus the minimal model predicts that the decay of glucose concentration during an IVGTT at basal insulin is monoexponential, with S_G as rate constant. The fractional decay rate of incremental glucose concentration (k_G , min^{-1}), namely the fraction of glucose concentration above basal that declines per unit time, is constant and equal to S_G

$$k_G(t) = -\Delta \dot{g}(t)/\Delta g(t) = S_G \quad (7)$$

The true glucose system, however, is not monocompartmental. Using the two-compartment model presented in the previous section, one can show (APPENDIX D) that glucose decay during an IVGTT at basal insulin is described by two exponentials

$$\Delta g(t) = D(A_1 e^{-\lambda_1 t} + A_2 e^{-\lambda_2 t}) \quad (8)$$

where λ_1 and λ_2 (min^{-1}) are the fast and slow components of glucose decay, respectively ($\lambda_1 > \lambda_2$). Because of the presence of two time constants, the fractional decay rate of incremental glucose concentration is no longer constant, but time varying

$$k_G(t) = -\Delta \dot{g}(t)/\Delta g(t) = \frac{A_1 \lambda_1 e^{-\lambda_1 t} + A_2 \lambda_2 e^{-\lambda_2 t}}{A_1 e^{-\lambda_1 t} + A_2 e^{-\lambda_2 t}} \quad (9)$$

In particular, $k_G(t)$ is higher at the beginning of the IVGTT, when the fast component of glucose decay (λ_1) plays an important role, and lower at the end of the IVGTT, when only the slow component (λ_2) remains in play.

We compared the glucose decay curves and the fractional decay rates of incremental glucose concentration predicted by the two-compartment and the minimal models, using for the two-compartment model the parameters of Table A1, and for the minimal model the S_G and V values reported in Table 2. Figure 6 shows the glucose decay curves (A) and the fractional decay rates of incremental glucose concentration (B) predicted by the two models. The monoexponential decay curve predicted by the minimal model and the two-exponential profile generated by the two-compartment model are almost superimposable in the period of minutes 10–20 of the IVGTT but diverge thereafter, thus reproducing closely the experimental observations by Quon et al. (30). Of note is that the value of S_G (0.021 min^{-1}) lies between the values that k_G takes on between 10 and 20 min [e.g., $k_G(\text{minute } 15) = 0.023 \text{ min}^{-1}$]. These results suggest that the validity of S_G as descriptor of the effect of glucose per se is confined to the initial portion of the IVGTT. The local validity of S_G is probably related to the fact that, during an IVGTT with

a normal insulin response, S_G estimation critically depends on the glucose data collected in the early portion of the IVGTT, when glucose concentration is high over the baseline and insulin action, albeit increasing, is still low (20). Because in that part of the test both components of glucose decay are active, S_G not only reflects glucose effects on R_d and EGP but also the rapid exchange of glucose between the accessible and the nonaccessible compartments occurring in the early part of the test.

Validation of S_G

Validation of S_G entails its comparison with the analogous index S_G measured with the glucose clamp method, $S_{G(\text{clamp})}$. In comparing S_G with $S_{G(\text{clamp})}$, one is faced with the problem that such indexes have different units: S_G is expressed in min^{-1} , whereas $S_{G(\text{clamp})}$ is expressed in $\text{ml} \cdot \text{kg}^{-1} \cdot \text{min}^{-1}$. As previously suggested in Ref. 17, to convert them to a common unit one has to multiply S_G by the minimal model volume of glucose distribution, V . The correctness of this approach has been formally demonstrated in Refs. 16 and 37. Of note is that V emerges from the minimal model method and can be individualized in each subject. In addition, multiplication of S_G by V parallels the approach used in the validation studies of S_I (10, 32).

The value of $S_G V$ found experimentally in the present study ($4.2 \text{ ml} \cdot \text{kg}^{-1} \cdot \text{min}^{-1}$) is much higher than the value of $S_{G(\text{clamp})}$ in normal subjects that can be found in the literature ($2.4 \text{ ml} \cdot \text{kg}^{-1} \cdot \text{min}^{-1}$ in Ref. 11). The same trend is observed if the value of $S_G V$ obtained from our Monte Carlo study is compared with the glucose effectiveness index of the two-compartment model (see Table 2). The reason for $S_G V$ being almost twice $S_{G(\text{clamp})}$ is that S_G and $S_{G(\text{clamp})}$ reflect different combinations of the fast and slow components of glucose disappearance at basal insulin, λ_1 and λ_2 . We have shown that S_G reflects the values that k_G takes on between 10 and 20 min. Thus, from Eq. 9, one has

$$S_G V = \left[\frac{(A_1 \lambda_1 e^{-\lambda_1 t_0} + A_2 \lambda_2 e^{-\lambda_2 t_0})}{(A_1 e^{-\lambda_1 t_0} + A_2 e^{-\lambda_2 t_0})} \right] V \quad (10)$$

where t_0 is ~ 15 min in subjects with a normal insulin response. Equation 10 shows that S_G is influenced by both the fast and slow components of glucose disappearance. To compare quantitatively $S_G V$ with $S_{G(\text{clamp})}$, it is useful to express S_G as a function of λ_2 only. By exploiting the fact that $A_1 \lambda_1 e^{-\lambda_1 t_0} \approx 2A_2 \lambda_2 e^{-\lambda_2 t_0}$ and $A_2 e^{-\lambda_2 t_0} \approx 6A_1 e^{-\lambda_1 t_0}$ (the values of A_1 , A_2 , λ_1 , and λ_2 reported in Table D1), one has

$$S_G V \approx 2.6 \lambda_2 V \quad (11)$$

$S_{G(\text{clamp})}$ is measured from a hyperglycemic glucose clamp in which somatostatin is used to suppress the endogenous insulin release, and the baseline insulin is replaced by an exogenous insulin infusion (11). By applying the formal definition of glucose effectiveness reported in Eq. C1 to a hyperglycemic clamp at basal insulin, one finds that $S_{G(\text{clamp})}$ is defined as the ratio of

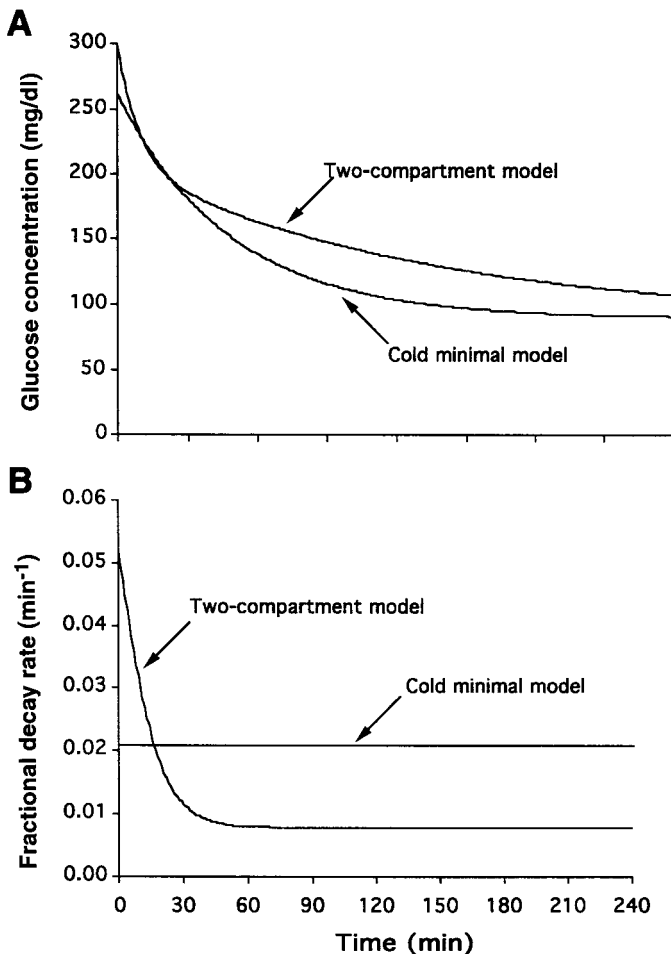


Fig. 6. Comparison between the two-compartment and the cold minimal model predictions of glucose concentration (A) and fractional decay rate of incremental glucose concentration (k_G , B) during an IVGTT at basal insulin. The value of S_G estimated during an IVGTT with a normal insulin response is close to the value of k_G in the initial portion of the test, approximately between 10 and 20 min.

$\Delta(R_d - \text{EGP})$ to the increment in plasma glucose concentration at steady state. Given that in the hyperglycemic steady state the increment in the exogenous glucose infusion rate, ΔGINF , equals $\Delta(R_d - \text{EGP})$, $S_{G(\text{clamp})}$ is defined as follows

$$S_{G(\text{clamp})} = \frac{\Delta(R_d - \text{EGP})}{\Delta g} \Big|_{i=i_b} = \frac{\Delta\text{GINF}}{\Delta g} \Big|_{i=i_b} \quad (12)$$

Using the two-compartment model to describe the glucose system during the clamp, one can express $S_{G(\text{clamp})}$ as a function of the parameters of the model and, specifically, of the two components of glucose disappearance at basal insulin (see derivation in APPENDIX E)

$$S_{G(\text{clamp})} = \frac{1}{\left(\frac{A_1}{\lambda_1} + \frac{A_2}{\lambda_2}\right)} \quad (13)$$

It is easy to show that $S_{G(\text{clamp})}$ is primarily determined by the slow component of glucose disappearance. In fact, $A_2/\lambda_2 \approx 18A_1/\lambda_1$, and thus $S_{G(\text{clamp})} \approx \lambda_2/A_2$. Moreover, because $1/A_2$ approximates the total glucose distribution volume V_T (28), and $V_T \approx 1.3V$ (see Tables 1 and A1), we can write

$$S_{G(\text{clamp})} \approx \lambda_2 V_T \approx 1.3\lambda_2 V \quad (14)$$

By comparing Eqs. 11 and 14, one realizes why S_{GV} is about twice $S_{G(\text{clamp})}$. It is worth pointing out that S_{GV} and $S_{G(\text{clamp})}$ are not only quantitatively, but also qualitatively different; S_{GV} also reflects, in addition to glucose effect on R_d and EGP [measured by $S_{G(\text{clamp})}$], the exchange process taking place between the two glucose compartments in the early part of the IVGTT. As a consequence, the correlation between these two indexes is unlikely to be strong, as suggested by the simulation studies reported in Refs. 22 and 38.

Finegood and Tzur have compared S_G with $S_{G(\text{clamp})}$ in dogs (24). To allow the comparison, the authors divided $S_{G(\text{clamp})}$ by the total volume of glucose distribution, V_T , taken from the literature (250 ml/kg). They found that S_G was higher than the ratio of $S_{G(\text{clamp})}$ to V_T and that such indexes were poorly correlated. These findings seem to support the notion that S_G and $S_{G(\text{clamp})}$ reflect different aspects of glucose effect per se. However, as we pointed out in Ref. 16, using V_T to convert $S_{G(\text{clamp})}$ to the same units as S_G is questionable because, as we have discussed, the minimal model yields an index of glucose effectiveness, S_{GV} , that has the same units of $S_{G(\text{clamp})}$ and hinges on a volume that, in contrast to a mean value of V_T , can be individualized in each subject.

S_G from an IVGTT at Basal Insulin

It is commonly believed that S_G estimated from an IVGTT at basal insulin is a reliable measure of glucose effectiveness, because under such conditions glucose is the only determinant of glucose decay. However, even under these optimized conditions, the validity of S_G is uncertain because the minimal model forces a monoexponential function to describe a two-exponential decay.

To determine whether S_G estimated from an IVGTT at basal insulin is a valid measure of glucose effectiveness, it is useful to recognize that, under such experimental conditions, a minimal model-independent index of glucose effectiveness can be calculated directly from the area under glucose decay. In fact in Ref. 4 we showed that whenever insulin concentration is maintained at the basal level and exogenous glucose forces glucose to increase and return to the baseline, glucose effectiveness at basal insulin, denoted as GE_b in Ref. 4, is given by the ratio between the administered amount of glucose and the area under the curve of the glycemic excursion above baseline [$\text{AUC}(\Delta g)$]. In the case of an IVGTT at basal insulin, with the assumption that glucose decay follows the two-exponential profile of Eq. 8, GE_b is given by

$$GE_b = \frac{D}{\text{AUC}[\Delta g(t)]} = \frac{1}{\left(\frac{A_1}{\lambda_1} + \frac{A_2}{\lambda_2}\right)} \quad (15)$$

Note that the expression of GE_b in Eq. 15 coincides with that of $S_{G(\text{clamp})}$ in Eq. 13, in keeping with the analysis carried out in Ref. 4 that ascertained the theoretical equivalence of these two measurements of glucose effectiveness. In that study (4), insulin was maintained at the basal level and glucose excursion was similar to that observed during a meal. Under those circumstances, S_{GV} resulted in a value similar to GE_b . It is presently unknown whether this also holds for an IVGTT at basal insulin, because during such an experiment the glucose profile is less smooth than during a meal, and the minimal model is unable to account for the rapid fall of glucose immediately after the glucose bolus. Nevertheless, some observations can be made. We have seen previously that, during an IVGTT with a normal insulin response, glucose decay reflects both glucose effectiveness and insulin action, and S_G is mainly estimated from the glucose data collected in the initial part of the IVGTT, when insulin action is still low. During an IVGTT at basal insulin, insulin action is null throughout the test, and glucose decay is governed by glucose effectiveness only. As a result, all of the glucose data between 10 min and the end of the test contribute to S_G estimation. Because the contribution of the fast component of glucose disappearance, λ_1 , soon becomes negligible (e.g., after ~ 30 min in normal subjects), and most of the glucose data are beyond that point in time, S_G will approach the slow component of glucose disappearance, λ_2 , and the minimal model volume will approach the reciprocal of A_2 . Therefore, S_{GV} is approximated by

$$S_{GV} \approx \frac{\lambda_2}{A_2} \quad (16)$$

Comparison of Eq. 16 with Eqs. 10 and 11 sheds some light on the reasons why the value of S_G obtained from an IVGTT at basal insulin has been found to be lower than that obtained from an insulin-modified IVGTT (24): whereas the S_G estimated during an insulin-

modified IVGTT reflects both the fast and slow components of glucose disappearance, the S_G estimated from an IVGTT at basal insulin reflects primarily the slow component. Comparison of *Eqs. 15* and *16* indicates that, during an IVGTT at basal insulin, S_{GV} will be close to GE_b if $A_2/\lambda_2 \gg A_1/\lambda_1$. Because $A_2/\lambda_2 \approx 18A_1/\lambda_1$, it is likely that S_{GV} estimated from an IVGTT at basal insulin is a reliable estimate of glucose effectiveness.

S_G measured from an IVGTT at basal insulin has been compared with $S_{G(\text{clamp})}$ in dogs by Finegood and Tzur (24). They found similar values for S_G and $S_{G(\text{clamp})}$ but no correlation between them. Whereas the agreement between the mean values of the two indexes is consistent with the above analysis, the absence of correlation between them is surprising. In fact, this would mean that the minimal model is not able to accurately assess glucose effectiveness, even when the IVGTT is performed at basal insulin. As pointed out in Ref. 16, one possible explanation for this finding is the relatively narrow range of glucose effectiveness observed in the group of dogs examined in that study. Another possible explanation is related to the fact that, at the end of the IVGTT studies carried out at basal insulin, glucose concentration was below the pretest level and still declining. This outcome may be due to the difficulty of obtaining a stable baseline for glucose concentration with the combined somatostatin, glucagon, and insulin infusion protocol. Alternatively, it could be the symptom of an inaccurate description of EGP in the minimal model. In fact, the model assumes that any change in glucose concentration is accompanied by a proportional and opposite change in EGP. The time course of EGP during an IVGTT at basal insulin is thus expected to mirror that of glucose concentration. However, the finding that at the end of the IVGTT glucose concentration was below the pretest level and still declining suggests that EGP was still inhibited at that time, implying that the minimal model description is not correct. This model inadequacy may have affected the accuracy of S_G and worsened its concordance with $S_{G(\text{clamp})}$.

COLD INSULIN SENSITIVITY

Effects of Monocompartmental Undermodeling on S_I

The monocompartmental approximation also influences the minimal model estimates of insulin action and sensitivity. As shown in Ref. 18, because the model has to compensate for S_G overestimation and fit the glucose data, insulin action is underestimated approximately until glucose returns to the baseline and is overestimated thereafter. This bias also affects S_I , because this parameter can be expressed as the ratio between the AUCs of insulin action and insulin concentration above basal level (18). Here we build on that paper and analyze the bias affecting the minimal model insulin action and S_I by comparing them with the insulin action and sensitivity of the two-compartment model. In carrying out this comparison, one must bear in mind that the cold model insulin action, $x(t)$, represents the sum of the insulin effects on glucose uptake

and production. In the two-compartment model, $x_d(t)$ is insulin action on glucose uptake, and $x_p(t)$ is insulin action on production. Thus $X(t) = x_p(t) + x_d(t)$ represents exactly what $x(t)$ represents for the minimal model. The profiles of $X(t)$ and $x(t)$ during a standard IVGTT are compared in Fig. 7A. $X(t)$ was generated using the two-compartment model parameters reported in Table A1; $x(t)$ was generated using the mean parameters S_I and p_2 estimated with the Monte Carlo simulation described in APPENDIX B ($S_I = 2.9 \times 10^{-4} \text{ min}^{-1} \cdot \mu\text{U}^{-1} \cdot \text{ml}$ and $p_2 = 0.027 \text{ min}^{-1}$). It can be seen that the minimal model markedly underestimates insulin action during the first half of the test and slightly overestimates it thereafter. It must be recognized, however, that this bias originates not only from the different model order (one vs. two pools) but also from the different location of insulin action on glucose uptake (accessible vs. non-accessible pool). To single out the effect of monocompartmental undermodeling per se, we calculated in APPENDIX F the effect that $x_d(t)$ produces on the accessible pool of the two-compartment model. We termed this effect as $\tilde{x}(t)$. $\tilde{X}(t) = x_p(t) + \tilde{x}(t)$ is therefore the “accessible-pool equivalent” insulin action of the two-compartment model that produces the same effect as X on plasma glucose concentration (i.e., the accessible-pool R_d remains the same). $\tilde{X}(t)$ is shown in Fig. 7B plotted against the insulin action of the minimal model. Qualitatively speaking, $\tilde{X}(t)$ is a delayed and blunted version of $X(t)$.

The difference $\Delta_x(t) = \tilde{X}(t) - x(t)$ represents the effect of monocompartmental undermodeling on the minimal model insulin action. $\Delta_x(t)$ can be analyzed theoretically by assuming that the minimal model fit of IVGTT glucose concentration is perfect. In this case an analytic expression for $\Delta_x(t)$ can be derived (details in APPENDIX F) that helps to single out the determinants of the bias

$$\begin{aligned} \Delta_x(t) &= \tilde{X}(t) - x(t) \\ &= - \left[\left(\frac{GE}{V_1} - S_G \right) \frac{\Delta g(t)}{g(t)} + \frac{\gamma}{(k_{22})^2} \frac{\dot{g}_2(t)}{g(t)} \right] \quad (17) \end{aligned}$$

where GE/V_1 is the fractional glucose effectiveness of the two-compartment model, $\gamma = k_{21}k_{12}$ and $k_{22} = (k_{02} + k_{12})$, and $\tilde{g}_2(t)$ is glucose concentration in the nonaccessible pool when insulin-dependent glucose removal occurs in the accessible pool.

The question arises as to what extent the analytic expression of $\Delta_x(t)$ derived under the assumption of perfect minimal model fit agrees with the profile of $\Delta_x(t)$ calculated by subtracting the profiles of $x(t)$ and displayed in Fig. 7B [note that $x(t)$ has been estimated from simulated, but realistic, IVGTT data and thus reflects a realistic, but not perfect, minimal model fit]. The two profiles of $\Delta_x(t)$ are compared in Fig. 7C. They agree closely, indicating that *Eq. 17* provides a good description of this difference. The only discrepancy occurs in the initial portion of the IVGTT. This is not surprising, because the analytic $\Delta_x(t)$ is calculated in the hypothesis of perfect minimal model fit. In contrast, it is well-known that the minimal model is unable to fit the initial rapid decay of glucose and that the glucose

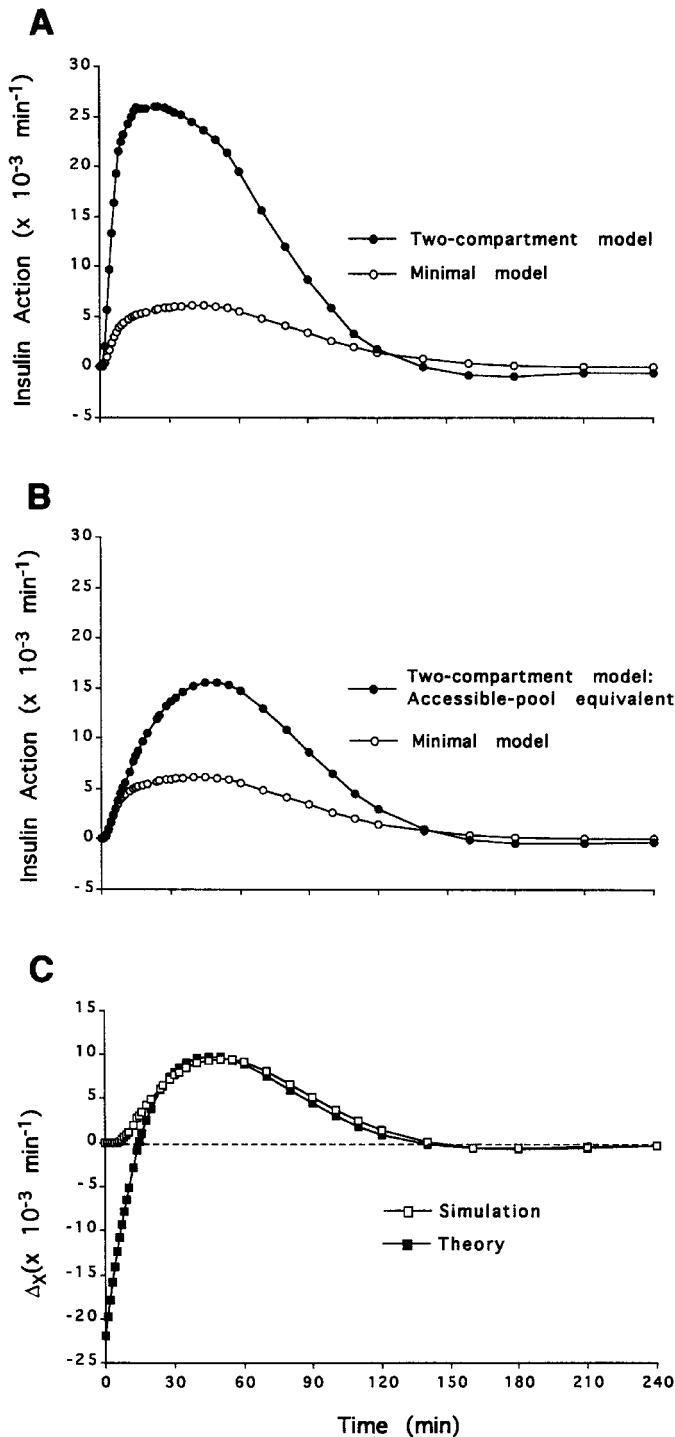


Fig. 7. *A*: comparison between insulin action of the two-compartment and the cold minimal models during a standard IVGTT. *B*: insulin action of the two-compartment model, which, if applied to the accessible pool, would produce the same effect on glucose concentration as the one taking place in the nonaccessible pool. This "accessible-pool equivalent" profile of the two-compartment insulin action is contrasted with the cold minimal model insulin action. *C*: difference between insulin action profiles of *B* is the effect of monocompartmental undermodeling on cold minimal model insulin action. This difference is shown against its analytically predicted time course.

data collected in the first 10 min of the test are not used in model identification. Thus from 10 min on we can use with confidence Eq. 17 to gain insight into the sources of the bias affecting the minimal model insulin action. It can be seen that Δ_x depends not only on S_G overestimation of the fractional glucose effectiveness of the two-compartment model ($GE/V_1 = 0.0133 \text{ min}^{-1}$) but also on the dynamics of glucose in the second glucose compartment. The first component of $\Delta_x(t)$, i.e., the bias affecting the estimate of glucose effectiveness ($S_G - GE/V_1$), is weighted by the term $\Delta g(t)/g(t)$. Such a function of time has a shape resembling that of plasma glucose decay and changes its sign when glucose exhibits an undershoot below its basal level. The second component, depending on glucose dynamics in the nonaccessible pool, is the major determinant of $\Delta_x(t)$. In fact, $\Delta_x(t)$ becomes positive at 20 min, i.e., approximately when $\tilde{g}_2(t)$ achieves its maximum, and returns negative at 140 min, just when $\tilde{g}_2(t)$ achieves its minimum. This implies that the bias affecting insulin action cannot be obviated completely by forcing S_G to assume a more accurate value.

The bias of insulin action obviously affects S_I . The difference between the fractional insulin sensitivity of the two-compartment model (IS/V_1) and S_I is given by Eq. F7 in APPENDIX F

$$\Delta_{S_I} = \frac{IS}{V_1} - S_I \approx \frac{\text{AUC}[\Delta_x(t)]}{\text{AUC}[i(t) - i_b]} \quad (18)$$

Equation 18 indicates that the bias of S_I depends on the whole time course of insulin action, so that compensations may occur between portions of the IVGTT when Δ_x is positive and portions when Δ_x is negative. Thus overestimation of S_G does not necessarily imply that S_I is underestimated, as recently pointed out (18, 24). However, because in our simulation study the AUC of underestimation is much greater than the AUC of overestimation, S_I underestimates the fractional insulin sensitivity of the two-compartment model by 55% (see Tables 1, 2, and A1). When S_I is multiplied by the minimal model volume, V , to allow comparison with IS (10, 32), underestimation reduces to 43% because V is higher than V_1 . Another observation is that the bias affecting S_I may be scarcely influenced by the value assumed by S_G , especially during a modified IVGTT in normal subjects. In fact, under such experimental conditions and in such a group of people, the integral of $\Delta g(t)/g(t)$ in Eq. 17 is very small, because the little but prolonged undershoot of glucose below its basal level due to the second insulin peak at 20 min gives rise to a negative AUC that balances the positive area associated with the rapid decline of glucose during the 1st h of the test. Because the integral of $\Delta g(t)/g(t)$ measures the effect that a unit change in S_G produces on S_I , it is likely that the sensitivity of S_I to errors in S_G is small.

One may wonder whether the underestimation of S_I may be mitigated by modifying the insulin profile during the IVGTT. This could happen, because insulin dynamics during the IVGTT affects both the numerator

and the denominator of Eq. 18. The impact on the denominator is obvious; that on the numerator is due to the fact that the insulin profile influences the time course of glucose concentration in both the glucose pools, thus producing an effect on $AUC[\Delta_x(t)]$ as well (see Eq. 17). The Monte Carlo simulation results of Table 1 suggest that the modified IVGTT slightly mitigates the bias of S_I . In fact, $S_I V$ underestimation with respect to IS reduces to 37%. Thus the modified IVGTT favors not only a greater precision (40) but also a greater accuracy of S_I . In our simulation the improvement of S_I accuracy was primarily due to the increment in $AUC[i(t) - i_b]$. In fact, although the added burst of insulin steepened the glucose curve, thus making $\Delta_x(t)$ less sluggish than during the standard IVGTT, $AUC[\Delta_x(t)]$ did not change much.

One final remark concerns the effect of monocompartmental undermodeling on the estimation of S_I in non-insulin-dependent diabetes mellitus (NIDDM). Many reports have shown that S_I estimated from an insulin-modified IVGTT in NIDDM patients is often imprecise and poorly correlated with the index calculated with the glucose clamp (3, 32). These problems can be interpreted, at least in part, in the light of the above-mentioned effects of single-compartment undermodeling on insulin action and S_I . The true insulin action in NIDDM patients is presumably very low because this group is markedly resistant to insulin. The error due to monocompartmental undermodeling can cause the minimal model insulin action to become so low and slow as to degrade the precision of S_I . In addition, even when S_I can be precisely estimated, its value will be markedly underestimated. Underestimation of S_I will further narrow the range of the minimal model estimates of insulin sensitivity in this group, thus worsening the correlation with the clamp-based measure of insulin sensitivity.

Validation of S_I

Validation of S_I entails its comparison with $S_{I(\text{clamp})}$, i.e., the glucose clamp measure of insulin sensitivity. By applying the formal definition of insulin sensitivity reported in Eq. C3 to a euglycemic, hyperinsulinemic clamp, one finds that $S_{I(\text{clamp})}$ is the steady-state ratio of $\Delta(R_d - \text{EGP})$ to the increment in plasma insulin concentration, normalized to the ambient plasma glucose concentration at which the clamp is performed. Because in the hyperinsulinemic steady state the increment in the exogenous glucose infusion rate equals $\Delta(R_d - \text{EGP})$, $S_{I(\text{clamp})}$ is defined as follows (7, 10, 32)

$$S_{I(\text{clamp})} = \frac{\Delta(R_d - \text{EGP})}{g\Delta i} \Big|_{g=\text{gb}} = \frac{\Delta \text{GINF}}{g\Delta i} \Big|_{g=\text{gb}} \quad (19)$$

To compare S_I with $S_{I(\text{clamp})}$, S_I is usually multiplied by the glucose distribution volume of the minimal model, V (10, 32). $S_I V$ and $S_{I(\text{clamp})}$ are well correlated, especially in normotolerant subjects, when the IVGTT is modified with the injection of either tolbutamide or insulin (5, 10, 32). Are they also equivalent measures of

insulin sensitivity, i.e., is their regression line indistinguishable from the unity line (slope = 1, intercept = 0)? Equivalence between $S_I V$ and $S_{I(\text{clamp})}$ is controversial in the literature.

In the study by Beard et al. (5) in normotolerant subjects, S_I was measured with the tolbutamide-modified IVGTT, and $S_{I(\text{clamp})}$ was measured with sequential low-insulin-dose euglycemic clamps, bringing insulin to plateaus of 21 and 35 $\mu\text{U}/\text{ml}$. A strong correlation between S_I and $S_{I(\text{clamp})}$ was found ($r = 0.84$). However, if one calculates the product $S_I V$ [using for V a typical value of 170 ml/kg (10, 17)], one finds that $S_I V$ was approximately 60% lower than $S_{I(\text{clamp})}$ (0.11 vs. 0.29 $\text{ml} \cdot \text{kg}^{-1} \cdot \text{min}^{-1} \cdot \mu\text{U}^{-1} \cdot \text{ml}$).

Bergman et al. (10) compared $S_I V$ and $S_{I(\text{clamp})}$ in a group of normotolerant and obese subjects. $S_I V$ was measured with the tolbutamide-modified IVGTT, and $S_{I(\text{clamp})}$ was measured with low- and high-insulin-dose euglycemic clamps carried out on different days. Insulin levels were 41 and 114 $\mu\text{U}/\text{ml}$, thus higher than in Ref. 5. Although $S_I V$ was slightly lower than $S_{I(\text{clamp})}$ in all subjects but one, $S_I V$ was equivalent to $S_{I(\text{clamp})}$ (0.046 vs. 0.052 $\text{dl} \cdot \text{min}^{-1} \cdot \mu\text{U}^{-1} \cdot \text{ml}$, respectively).

Saad et al. (32) compared $S_I V$ with $S_{I(\text{clamp})}$ in normal controls, subjects with impaired glucose tolerance (IGT), and patients with NIDDM. S_I was measured with the insulin-modified IVGTT (insulin bolus of 0.03 U/kg at 20 min), while $S_{I(\text{clamp})}$ was measured with a single high-insulin-dose euglycemic clamp, bringing insulin levels to 83 $\mu\text{U}/\text{ml}$. Although results show $S_I V$ and $S_{I(\text{clamp})}$ well correlated in normal and IGT subjects, $S_I V$ was >50% lower than $S_{I(\text{clamp})}$.

More recently, Saad et al. (33) measured $S_I V$ in normal controls with both the tolbutamide- and the insulin-modified IVGTT, while $S_{I(\text{clamp})}$ was measured with the same insulin infusion used in Ref. 32. $S_I V$ from the tolbutamide-modified IVGTT was only 13% lower than $S_{I(\text{clamp})}$ (0.045 vs. 0.054 $\text{dl} \cdot \text{min}^{-1} \cdot \mu\text{U}^{-1} \cdot \text{ml}$), whereas $S_I V$ from the insulin-modified IVGTT (0.030 $\text{dl} \cdot \text{min}^{-1} \cdot \mu\text{U}^{-1} \cdot \text{ml}$) was 44% lower than $S_{I(\text{clamp})}$.

Comparison of the results obtained in the above-mentioned studies suggests that equivalence of $S_I V$ and $S_{I(\text{clamp})}$ depends on how the IVGTT and the clamp are performed. For instance, the marked difference between $S_I V$ and $S_{I(\text{clamp})}$ that is present when either $S_I V$ is estimated from an insulin-modified IVGTT (32) or $S_{I(\text{clamp})}$ is estimated from low-dose insulin clamps (5) vanishes when $S_I V$ is estimated from a tolbutamide-boostered IVGTT and $S_{I(\text{clamp})}$ is derived from high-dose insulin clamps (10, 33). To understand the reasons for this protocol dependency, it is useful to examine the hypotheses governing the assessment of S_I and $S_{I(\text{clamp})}$. For S_I to be equivalent to $S_{I(\text{clamp})}$, a number of conditions must be met, the most important of which are that 1) the minimal model single-pool description of glucose kinetics is adequate; 2) insulin effect on the aggregation of R_d and EGP increases linearly with insulin concentration across the insulin range experienced during the IVGTT and the clamp; 3) insulin sensitivity is independent from the route of insulin delivery (portal

vs. peripheral); and 4) tolbutamide has no effects per se on glucose metabolism. We have already shown that monocompartmental undermodeling leads to S_I underestimation. We now analyze how the other factors can influence the estimation of S_I and $S_{I(\text{clamp})}$.

Linearity of insulin effect. Both S_I and $S_{I(\text{clamp})}$ measure the ability of insulin not only to increase R_d but also to inhibit EGP. Therefore, both such aspects of insulin action are important in determining overall insulin sensitivity. In glucose clamp studies, insulin levels are brought to ~ 40 and $100 \mu\text{U/ml}$ during either low- or high-dose insulin clamps. Whereas the steady-state relationship between R_d and insulin concentration is approximately linear in the physiological range ($10\text{--}100 \mu\text{U/ml}$) (7), the relationship between EGP and insulin concentration is highly nonlinear in the same range, because EGP achieves nearly complete suppression at insulin levels of $\sim 40 \mu\text{U/ml}$ (26), so that any further increment in insulin concentration is not accompanied by a proportional decrement in EGP. Evidence that the nonlinearity of the relationship between insulin concentration and EGP suppression is likely to affect the measurement of $S_{I(\text{clamp})}$ can be derived from the study of Katz et al. (26). The data reported in that dose-response study allow calculation of $S_{I(\text{clamp})}$ at three insulin levels: 25, 43, and $123 \mu\text{U/ml}$. $S_{I(\text{clamp})}$ shows results of 0.19, 0.21, and $0.10 \text{ ml} \cdot \text{kg}^{-1} \cdot \text{min}^{-1} \cdot \mu\text{U}^{-1} \cdot \text{ml}$, respectively. These values indicate that $S_{I(\text{clamp})}$ is independent of the insulin level until EGP reaches nearly complete suppression at $\sim 40 \mu\text{U/ml}$. As the insulin level increases beyond that point, any further increase in insulin action will depend solely on an increase in R_d . That $S_{I(\text{clamp})}$ depends on the insulin level at which the clamp is performed can also be inferred by comparing the values of $S_{I(\text{clamp})}$ in normal subjects obtained in the studies by Beard et al. (5) and Saad et al. (32). $S_{I(\text{clamp})}$ was $0.29 \text{ ml} \cdot \text{kg}^{-1} \cdot \text{min}^{-1} \cdot \mu\text{U}^{-1} \cdot \text{ml}$ in Ref. 5, in which insulin levels were 21 and $35 \mu\text{U/ml}$, but $0.10 \text{ ml} \cdot \text{kg}^{-1} \cdot \text{min}^{-1} \cdot \mu\text{U}^{-1} \cdot \text{ml}$ in Ref. 32, in which insulin level was $83 \mu\text{U/ml}$. All in all, these data suggest that when $S_{I(\text{clamp})}$ is derived from a high-dose insulin clamp, it will tend to underestimate insulin effect on EGP.

During an IVGTT, because of the dynamic nature of the test, what really matters is the insulin level attained in the remote insulin compartment from which insulin action is exerted. During a standard or a tolbutamide-boostered IVGTT, plasma insulin levels rarely exceed $200 \mu\text{U/ml}$, and insulin action is likely to remain within the quasi-linear range. The risk of entering into the nonlinear range of insulin action increases during an insulin-modified IVGTT in which peak insulin levels as high as $400\text{--}600 \mu\text{U/ml}$ are elicited by a bolus or a short infusion of exogenous insulin. As a matter of fact, a recent report by Vicini et al. (39) suggests that saturation of insulin effect on EGP is likely to take place during an insulin-modified IVGTT. In that study (39), the time course of EGP during an insulin-modified IVGTT was accurately assessed by using the tracer-to-tracee (specific activity)

clamp. EGP achieved almost complete suppression at 20 min and remained suppressed for another 20 min after the exogenous insulin administration. We speculate that, because between 20 and 40 min the high insulin levels due to the exogenous insulin injection cannot produce any further inhibition in EGP, insulin effect on EGP is underestimated in that interval. It seems, however, that this transient saturation of insulin effect on EGP (and possibly on R_d) is unable to influence S_I appreciably (comprising both the effects of insulin on R_d and EGP). In fact, recent results provided by Saad et al. (34), contradicting a previous report by Prigeon et al. (29), indicate that the estimate of S_I is not appreciably influenced by the peak insulin level achieved during an insulin-modified IVGTT in which insulin is administered either as a bolus or as an equidose short infusion.

Portal vs. peripheral route of insulin delivery. In comparing S_I with $S_{I(\text{clamp})}$, we assume that the peripheral and portal routes of insulin delivery are equally effective in inhibiting EGP. Unlike $S_{I(\text{clamp})}$, which measures insulin ability to suppress EGP and elevate R_d in response to peripheral insulin delivery, S_I is estimated from insulin and glucose profiles in response to either portally delivered insulin (during a standard or a tolbutamide-modified IVGTT) or to a mixture of portally and peripherally appearing insulin (during an insulin-modified IVGTT). Recently, Steil et al. (35) studied the contribution of portal insulin to the assessment of S_I by performing paired insulin-modified IVGTTs in dogs in which insulin was infused either portally or peripherally with matched peripheral insulin levels. They found that portal insulin delivery does not significantly affect insulin's ability to normalize plasma glucose after the glucose bolus and that the route of insulin delivery does not appreciably affect S_I .

Effects of tolbutamide. Saad and colleagues (33, 34) have shown that the tolbutamide-boostered protocol provides higher S_I estimates than the insulin-modified protocol, regardless of the method of insulin administration (bolus or 5- or 10-min infusion). The higher S_I values from the tolbutamide protocol cannot be explained by differences in peripheral insulinemia, because giving insulin as a 10-min infusion results in peripheral insulin levels similar to those measured after tolbutamide (34). In addition, the aforementioned study by Steil et al. (35) seems to rule out the possibility that this difference is due to the effect of higher portal concentrations seen after tolbutamide but not insulin injection. Saad et al. (34) hypothesized that tolbutamide-induced proinsulin release during the IVGTT could play a role in elevating the estimates of S_I with the tolbutamide protocol with respect to those obtained with the insulin protocol. Alternatively, differences in S_I between tolbutamide- and insulin-modified IVGTTs could be due to some extrapancreatic effect of tolbutamide, as recently suggested (31). Whatever the case, the injection of tolbutamide contributes to elevate S_I with respect to $S_{I(\text{clamp})}$.

HOT GLUCOSE EFFECTIVENESS

*Effect of Monocompartmental Undermodeling on S_G^**

To study the effect of the monocompartmental approximation on S_G^* , we will use the same rationale previously used for S_G , i.e., we will first analyze the decay of hot glucose during a hot IVGTT in which insulin is maintained at the basal level. The minimal model predicts that the decay of hot glucose concentration is monoexponential, with S_G^* as rate constant

$$g^*(t) = \frac{D^*}{V^*} e^{-S_G^* t} \quad (20)$$

Thus the fractional decay rate of the tracer will be constant and equal to S_G^*

$$k_G^*(t) = -\dot{g}^*(t)/g^*(t) = S_G^* \quad (21)$$

In contrast, the two-compartment model predicts that the hot glucose decay is described by an almost two-exponential profile (APPENDIX D)

$$g^*(t) = D^*(A_1^* e^{-\lambda_1^* t} + A_2^* e^{-\lambda_2^* t}) + \alpha(t) \quad (22)$$

where λ_1^* and λ_2^* ($\lambda_1^* > \lambda_2^*$, min^{-1}) are the fast and slow rate constants of glucose kinetics in the basal state, respectively, and the term $\alpha(t)$ accounts for the effect of hyperglycemia on glucose clearance. The corresponding fractional decay rate is no longer constant, and its time course is shown in Fig. 8. k_G^* is high at the beginning of the IVGTT, when the fast component of glucose kinetics plays a relevant role, shows a rapid decline followed by a slight undershoot due to $\alpha(t)$, and then increases slowly, getting closer and closer to λ_2^* .

During a hot IVGTT, S_G^* is primarily estimated in the final portion of the test, when both insulin and

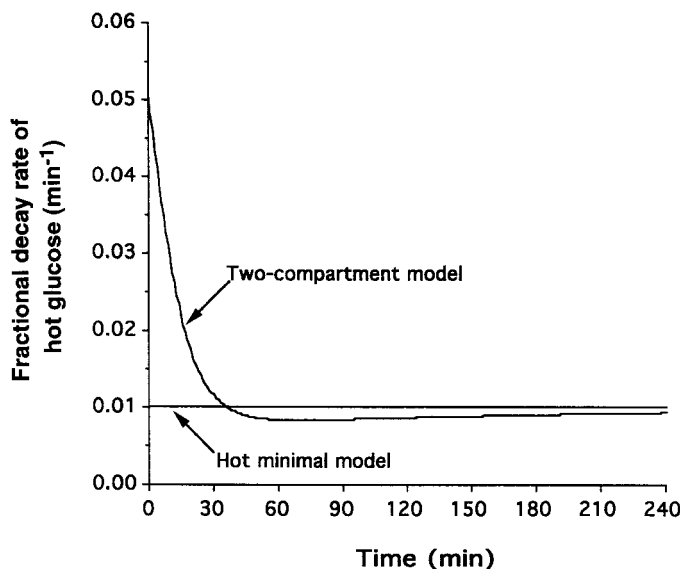


Fig. 8. Fractional decay rate of hot glucose (k_G^*) during a hot IVGTT at basal insulin. The value of S_G^* estimated during a hot IVGTT with a normal insulin response is close to the value of k_G^* in the final portion of the test.

glucose concentrations have almost returned to the baseline. At that point in time, both the contribution of the fast component of glucose kinetics and the inhibitory effect of hyperglycemia on glucose clearance have become negligible, and hot glucose decay is governed only by the slow component of glucose kinetics, λ_2^* . Thus, in the final part of the IVGTT, a single-pool description of glucose kinetics is adequate to describe hot glucose decay, and S_G^* approximates λ_2^* . As a matter of fact, by comparing Tables 1 and D1, one can see that the value of S_G^* estimated with the Monte Carlo simulation is close to λ_2^* ($S_G^* = 0.0102$ and 0.0098 min^{-1} from the standard and modified IVGTT, respectively, and $\lambda_2^* = 0.0093 \text{ min}^{-1}$). This agreement suggests that the domain of validity of S_G^* is confined to the final portion of the IVGTT. To clarify the physiological meaning of S_G^* , it is of interest to recall that the basal plasma clearance rate of glucose, PCR_b , is the inverse of the area under the hot glucose impulse response at basal insulin. The area can be expressed as a function of the eigenvalues of the two-exponential impulse response, as follows (13)

$$\text{PCR}_b = \frac{1}{\left(\frac{A_1^*}{\lambda_1^*} + \frac{A_2^*}{\lambda_2^*}\right)} \quad (23)$$

Given that $A_2^*/\lambda_2^* \sim 14A_1^*/\lambda_1^*$ (see Table D1), Eq. 23 reduces to

$$\text{PCR}_b \approx \lambda_2^*/A_2^* \quad (24)$$

Because S_G^* approximates λ_2^* and $1/A_2^*$ approximates V_T (28), one has

$$S_G^* \approx \frac{\text{PCR}_b}{V_T} \quad (25)$$

Therefore, S_G^* measures the ratio of glucose clearance and total distribution volume, i.e., basal fractional glucose clearance rate. In fact, if the S_G^* found experimentally in this study (0.0082 min^{-1}) is multiplied by a total volume of glucose distribution taken from the literature (260 ml/kg), one obtains $2.03 \text{ ml} \cdot \text{kg}^{-1} \cdot \text{min}^{-1}$, which agrees with the values of the basal plasma clearance rate found in the literature. The same trend is observed if S_G^* estimated from the Monte Carlo study is compared with the ratio between the plasma clearance rate and the total distribution volume of the two-compartment model ($S_G^* = 0.0102$ and 0.0098 min^{-1} from the standard and modified IVGTT, respectively, and $\text{PCR}/V_T = 0.0096 \text{ min}^{-1}$). The reliability of S_G^* as a descriptor of the basal fractional glucose clearance has been assessed in dogs by comparing S_G^* with the basal glucose clearance rate independently measured by the arteriovenous technique (19).

*Validation of S_G^**

In the hot minimal model, it is assumed that glucose uptake is proportional to glucose concentration. As a result, glucose clearance and glucose effectiveness on glucose disposal coincide in the model (see Table C1).

However, it is a well-established notion that glucose uptake is not proportional to glucose concentration and that, in the range of interest, the R_d vs. g relationship can be approximated by a line that has a nonzero intercept with the R_d axis (6, 11, 12, 36). As a consequence, glucose clearance and glucose effectiveness on glucose disposal do not coincide. In this section we clarify the relationship existing between S_G^* and the clamp estimate of glucose effectiveness on glucose disposal, $S_{G,d(\text{clamp})}$. $S_{G,d(\text{clamp})}$ is measured from hyperglycemic glucose clamp studies at basal insulin in which exogenous glucose is used to progressively increase glucose concentration, g , at various steady state levels, and a tracer is concurrently infused to measure R_d (12). By applying the definition of hot glucose effectiveness reported in Eq. C2 to a hyperglycemic clamp at basal insulin, one finds that $S_{G,d(\text{clamp})}$ is the slope of the linear relationship between the R_d and g

$$R_d = S_{G,d(\text{clamp})}g + R_{d,0} \quad (26)$$

where $R_{d,0}$ is the nonzero intercept. Recalling that S_G^* measures fractional basal glucose clearance (Eq. 25), and using the definition of basal glucose clearance (Eq. C5), one has

$$S_G^* V_T \approx \text{PCR}_b = \frac{R_{db}}{g_b} \quad (27)$$

Combining Eqs. 26 and 27 yields

$$S_G^* V_T \approx S_{G,d(\text{clamp})} + \frac{R_{d,0}}{g_b} \quad (28)$$

Equation 28 confirms that S_G^* does not coincide with $S_{G,d(\text{clamp})}$ (apart from the volume factor) because of the presence of the nonzero intercept $R_{d,0}$. Thus S_G^* cannot be used as an index of glucose effectiveness unless the presence of $R_{d,0}$ is explicitly taken into account in the hot minimal model. In a recent paper investigating glucose effectiveness during a meal-like study (4), the hot minimal model was modified to allow for the presence of $R_{d,0}$. Both S_G^* and $R_{d,0}$ were estimated from the data, because the basal plasma clearance rate was available in each subject, thanks to a pretest tracer equilibration experiment. It is worth noting that this pretest tracer experiment is not commonly performed before the IVGTT, and this makes the simultaneous estimation of S_G^* and $R_{d,0}$ from hot IVGTT data extremely difficult (17).

S_G vs. S_G^*

The analysis of the relationships S_G vs. $S_{G(\text{clamp})}$ and S_G^* vs. $S_{G,d(\text{clamp})}$ suggests a possible explanation for the lack of correlation between S_G and S_G^* found in this study. One would expect to find a good correlation between S_G and S_G^* because glucose clamp studies have shown that glucose effectiveness on R_d is the major determinant ($\sim 2/3$) of overall glucose effectiveness, with the remainder accounted for by the effect of glucose to inhibit EGP (11). However, as we have shown, S_G and S_G^* are not equivalent to $S_{G(\text{clamp})}$ and

$S_{G,d(\text{clamp})}$, respectively. In fact, S_G and $S_{G(\text{clamp})}$ measure related, but not identical, physiological processes, because S_G , at variance with $S_{G(\text{clamp})}$, is markedly influenced by the rapid exchange of glucose that takes place between the accessible and nonaccessible compartments after the glucose bolus. Likewise, S_G^* measures the fractional basal glucose clearance rate, but not glucose effectiveness on R_d , because the hot model does not account for the inhibitory effect of glucose on its own clearance.

HOT INSULIN SENSITIVITY

*Effects of Monocompartmental Undermodeling on S_I^**

The estimation of S_I^* suffers from problems that, to some extent, are opposite to those affecting S_I . Because S_G^* approximates the slow time constant of glucose kinetics at basal insulin, the minimal model tends to underestimate the rate of hot glucose decay per se (independently of insulin) during the early portion of the IVGTT, when the fast component of glucose kinetics plays an important role. To compensate for this underestimation and to fit hot glucose data, the hot minimal model insulin action is probably overestimated in the initial part of the IVGTT. To verify this hypothesis, we compared the insulin action on glucose disposal of the two-compartment model, $x_d(t)$, with the hot minimal model insulin action, $x^*(t)$ (Fig. 9A). The latter profile is generated using the mean parameters S_I^* and p_2^* estimated by Monte Carlo simulation ($S_I^* = 3.2 \times 10^{-4} \text{ dl} \cdot \text{kg}^{-1} \cdot \text{min}^{-1} \cdot \mu\text{U}^{-1} \cdot \text{ml}$ and $p_2^* = 0.069 \text{ min}^{-1}$). As argued in comments concerning cold insulin action, the difference between these profiles does not reflect only the different model order but also the different location of insulin action in the two models. Thus, to single out the effect of monocompartmental undermodeling per se, we calculated in APPENDIX F the effect that $x_d(t)$ produces on hot glucose concentration in the accessible pool of the two-compartment model. This “accessible-pool equivalent” profile of insulin action on glucose disposal, $\bar{x}_d^*(t)$ (the asterisk denotes that it is derived from tracer data), is compared with $x^*(t)$ in Fig. 9B. One can see that the hot minimal model overestimates insulin action until ~ 30 min and underestimates it thereafter. The difference $\Delta_x^* = \bar{x}_d^* - x^*$ represents the effect of monocompartmental undermodeling on the insulin action of the hot minimal model. Δ_x^* can be given the following analytic expression in the hypothesis that the minimal model fit of hot glucose data is perfect (APPENDIX F)

$$\begin{aligned} \Delta_x^*(t) &= \bar{x}_d^*(t) - x^*(t) \\ &= - \left[\left(\frac{\text{GE}^*}{V_1} - S_G^* \right) + \frac{\gamma}{(k_{22})^2} \frac{\dot{g}_2^*(t)}{g^*(t)} + \frac{R_{d,0}}{V_1 g(t)} \right] \quad (29) \end{aligned}$$

where GE^*/V_1 is the fractional hot glucose effectiveness of the two-compartment model; \dot{g}_2^* is hot glucose concentration in the nonaccessible glucose pool when insulin-dependent glucose removal occurs in the accessible pool. Δ_x^* obtained from Eq. 29 is plotted in Fig. 9C against the profile of Δ_x^* obtained from the difference

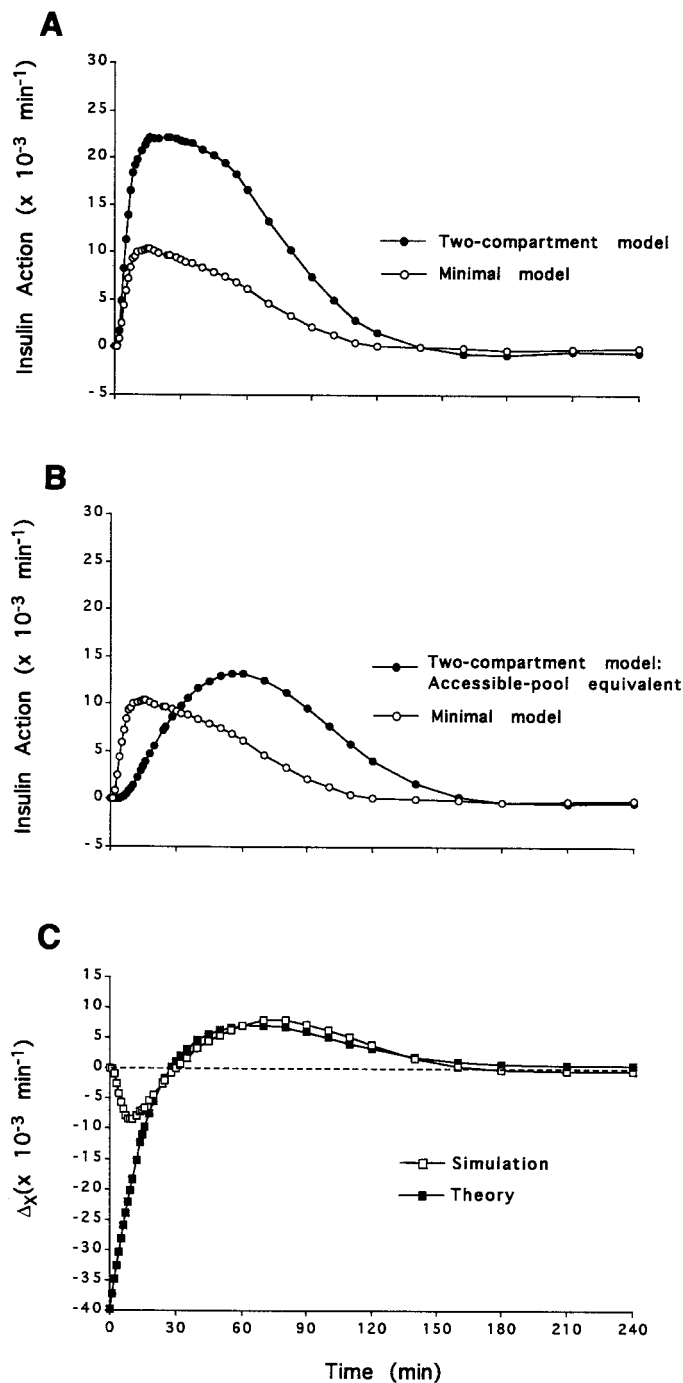


Fig. 9. *A*: comparison between insulin action on glucose disposal of two-compartment model and insulin action of hot minimal model during a standard hot IVGTT. *B*: insulin action of two-compartment model, which, if applied to the accessible pool, would produce the same effect on hot glucose concentration as the one taking place in the nonaccessible pool. This “accessible-pool equivalent” profile of two-compartment insulin action is contrasted with the hot minimal model insulin action. *C*: difference between insulin action profiles of *B* is the effect of monocompartmental undermodeling on hot minimal model insulin action. This difference is shown against its analytically predicted time course.

between the profiles of \hat{x}_d^* and x^* displayed in Fig. 9*B*. The two profiles agree closely except in the initial part of the test, because the hot model is unable to fit the initial rapid decay of hot glucose that follows the

glucose bolus. The structure of Δ_x^* resembles that of Δ_x (Eq. 17). In fact, Δ_x^* depends on the difference between the fractional glucose effectiveness of the two models and on the dynamics of hot glucose concentration in the nonaccessible pool; Δ_x^* also shows a term proportional to $R_{d,0}$ that accounts for the fact that the hot minimal model does not comprise a description of the inhibitory effect of glucose on its own clearance.

The bias affecting S_I^* can be calculated as previously done for S_I

$$\Delta_{S_I^*} = \frac{IS^*}{V_I} - S_I^* \approx \frac{\text{AUC}[\Delta_x^*(t)]}{\text{AUC}[i(t) - i_b]} \quad (30)$$

As for S_I , the bias of S_I depends on the whole time course of insulin action, so that compensations may occur between portions of the IVGTT when Δ_x^* is positive and others when Δ_x^* is negative. It can be calculated from Table 1 that S_I^* underestimates the fractional hot insulin sensitivity of the two-compartment model by 36%. When S_I^* is multiplied by the hot minimal model volume, V^* , to allow comparison with IS^* , underestimation reduces to ~15%. S_I^* underestimation can be mitigated by enhancing the insulin signal during the hot IVGTT. In fact, the Monte Carlo simulation results of Table 1 indicate that $S_I^*V^*$ calculated from an insulin-modified IVGTT is almost identical to IS^* .

One final remark concerns the ability of the hot minimal model to overcome the problems encountered with the cold minimal model in assessing insulin sensitivity in NIDDM patients. In Ref. 3 we have shown and explained why S_I^* can be precisely estimated even in those NIDDM patients in whom S_I cannot be estimated or is estimated with poor precision.

Validation of S_I^*

S_I^* has not yet been validated against the analogous clamp-based index $S_{I,d(\text{clamp})}$. However, S_I^* has been compared with the insulin sensitivity index yielded by the two-compartment minimal model developed in Ref. 14. Such a model, which explicitly accounts for glucose inhibition of glucose clearance, yields an insulin sensitivity index, S_I^{2*} , that is expressed in the same units as $S_{I,d(\text{clamp})}$ (37). $S_I^*V^*$ has been found to be similar and well correlated to S_I^{2*} (37). Although this agreement does not prove S_I^* accuracy, it suggests that monocompartmental undermodeling and the inadequate description of glucose effect on its own clearance do not bias $S_I^*V^*$ appreciably, presumably because of a reasonably good compensation between the initial overestimation and the subsequent underestimation of hot insulin action.

S_I vs. S_I^*

The error analysis of cold and hot insulin action and sensitivity explains the paradoxical finding $S_I < S_I^*$. In fact, whereas the underestimation affecting S_I is large, that affecting S_I^* is modest.

Also, the unexpected time lag between cold and hot insulin action may be due, at least in part, to a different effect of the monocompartmental approximation on the

insulin action of the two models. By comparing Figs. 7B and 9B, one can see that x is delayed with respect to the insulin action of the two-compartment model, whereas x^* is anticipated. This would provide a possible explanation of why parameter p_2 of the cold minimal model, which governs the speed of rise and decay of x , is systematically lower than the analogous hot parameter p_2^* .

CONCLUSIONS

The findings of the present paper can be summarized as follows.

S_G reflects the rate of glucose decay per se, independent of increased insulin, in the initial portion of the IVGTT, approximately between 10 and 20 min. It reflects not only the ability of glucose to promote R_d and inhibit EGP but also the rapid exchange of glucose that occurs between the two glucose compartments after the glucose bolus. Because the latter component of S_G is nonnegligible, as suggested by the simulation studies in Refs. 22 and 38, the reliability of S_G as descriptor of glucose effectiveness is uncertain.

The effects of single-compartment undermodeling on S_G determine undesired compensations on cold insulin action and S_I . Insulin action is markedly underestimated for a considerable portion of the IVGTT. S_I , which is proportional to the integral of insulin action, is also markedly underestimated. Although the S_I estimated from an insulin-modified or a tolbutamide-boostered IVGTT strongly correlates with $S_{I(\text{clamp})}$, it must be pointed out that both S_I and $S_{I(\text{clamp})}$ are protocol dependent and, in general, are not equivalent. In fact, besides the description of glucose kinetics (one vs. two compartments), other factors like nonlinearity of insulin action on EGP and effects of tolbutamide can influence their estimation.

S_G^* cannot be used as a descriptor of glucose effectiveness on glucose disposal unless an explicit description of the inhibitory effect of glucose on its own clearance is included in the hot model. Nevertheless, S_G^* has a clear-cut physiological interpretation, because it measures basal fractional glucose clearance.

Hot insulin action is influenced by monocompartmental undermodeling as well as by the hot model assumption that glucose has no effect on its own clearance. Hot insulin action is markedly overestimated in the initial portion of the IVGTT and is underestimated thereafter. S_I^* , which is proportional to the integral of hot insulin action, is only slightly underestimated, thus giving results more accurate than S_I . Although S_I^* has not yet been compared with the analogous clamp-based estimate of peripheral insulin sensitivity, it is well correlated to the estimate of insulin sensitivity provided by a physiological two-compartment minimal model (37).

The cold indexes S_G and S_I , but not the hot indexes S_G^* and S_I^* , suffer from an additional problem: their accuracy depends not only on the description of glucose kinetics (one vs. two compartments) but also on the reliability of the description of glucose and insulin control on EGP embodied in the cold model. This issue has not been examined in this article. Recently, the

tracer-to-tracee (specific activity) clamp has been used to estimate EGP in a model-independent fashion during an IVGTT (39). The resulting profile is not in agreement with the assumptions of the minimal model. However, it is difficult to single out the extent to which S_G and S_I are affected by this problem until a more reliable description of glucose and insulin control on EGP becomes available.

A two-compartment structure is the obvious way to go to anticipate and prevent monocompartmental undermodeling. As far as the hot minimal model is concerned, a two-compartment hot minimal model has been proposed that not only allows estimation of EGP by deconvolution (14, 39) but also yields metabolic indexes of glucose effectiveness, insulin sensitivity, and glucose clearance (37). The relationships between the indexes provided by the two-compartment and the single-compartment hot minimal models have been thoroughly examined in Ref. 37. The formulation of a cold two-compartment minimal model is far more difficult, because one is faced with a priori identifiability problems. Preliminary results (15) indicate that a two-compartment model can be resolved from cold IVGTT data if the available knowledge on the exchange kinetics between the accessible and nonaccessible glucose pools is incorporated in the model by a Bayesian approach. A possible alternative to mitigate the impact of monocompartmental undermodeling is to design experimental protocols that, at variance with the IVGTT, are characterized by more physiological glucose and insulin profiles, i.e., they are smoother than those observed during the IVGTT. This strategy has been pursued with success in Ref. 4, where the single-pool minimal models have interpreted cold and hot glucose data during an experiment in which insulin remained basal and glucose exhibited a prandial profile. Further studies are warranted to more fully explore both of these approaches.

APPENDIX A: TWO-COMPARTMENT SIMULATION MODEL OF THE IVGTT

Here we describe the two-compartment model used for simulating cold and hot glucose data during the hot IVGTT. Because cold glucose concentration is the result of the balance between R_d and EGP, both of these processes are described by the model. To describe R_d , we use a two-compartment model, which has been shown to provide a physiological description of glucose kinetics during the IVGTT (14, 37, 39). This model, shown in Fig. 5, has already been described in Refs. 14, 37, and 39; it builds on the two-compartment structure extensively analyzed in Ref. 21. Briefly, the accessible pool comprehends tissues that are in rapid equilibrium with plasma, like red blood cells, central nervous system, kidneys, and liver. These tissues consume glucose largely in an insulin-dependent way. The second pool comprehends tissues that equilibrate more slowly, with plasma, like muscle and fat. These tissues are mainly insulin dependent. This is the reason why in the model insulin-independent glucose disposal is assumed to take place in the accessible pool (*pool 1*), whereas insulin-dependent glucose disposal is assumed to occur in the nonaccessible pool (*pool 2*). Insulin-independent glucose uptake has two components, one constant and the other proportional to glucose concentration. Thus the fractional disappearance

rate of the accessible pool is

$$k_{01}(t) = k_d + \frac{R_{d,0}}{V_1 g(t)} \quad (A1)$$

where k_d accounts for the proportional term, and $R_{d,0}$ is the nonzero intercept of the steady-state relationship R_d vs. g . Because k_{01} decreases as glucose concentration increases, the model accounts for the well-known inhibitory effect of hyperglycemia on its own clearance (11, 12, 36).

Insulin-dependent glucose disposal is described by a parametric control on k_{02}

$$k_{02}(t) = k_{02} + x_d(t) \quad (A2)$$

where $x_d(t)$ is insulin action on glucose uptake originating from an insulin compartment remote from plasma. The dynamics of $x_d(t)$ is governed by parameters k_{bd} and k_a , which describe the transport of plasma insulin into the compartment and the removal of remote insulin from the compartment, respectively.

Physiological knowledge indicates that, in the basal state, one-fourth of glucose uptake is due to insulin-dependent glucose tissues and three-fourths to insulin-independent glucose tissues (21). This yields the following relationship among the parameters of the model

$$k_d + \frac{R_{d,0}}{g_b V_1} = \frac{3k_{21}k_{02}}{k_{02} + k_{12}} \quad (A3)$$

The model description of EGP during the IVGTT employs the same functional description embodied in the cold minimal model (8, 17, 19, 23). In fact, inhibition of EGP is assumed to be proportional to the glucose excursion above basal and to the product of glucose concentration and insulin action on EGP, $x_p(t)$, assumed to occur with the same timing as insulin action on R_d . This is the reason why the remote insulin compartments from which $x_p(t)$ and $x_d(t)$ originate have the same rate constant, k_a . In contrast, parameters k_{bd} and k_{bp} are different, with k_{bd} being higher than k_{bp} , because it is known from clamp studies that insulin effect is greater on R_d than on EGP.

The model equations for cold and hot glucose are

$$\begin{aligned} \dot{q}_1(t) &= - \left[k_d + \frac{R_{d,0}}{q_1(t)} + k_{21} \right] q_1(t) + k_{12} q_2(t) + \text{EGP}(t) & q_1(0) &= D + q_{1b} \\ \dot{q}_2(t) &= - [k_{02} + x_d(t) + k_{12}] q_2(t) + k_{21} q_1(t) & q_2(0) &= q_{1b} [k_{21} / (k_{02} + k_{12})] \\ \dot{q}_1^*(t) &= - \left[k_d + \frac{R_{d,0}}{q_1^*(t)} + k_{21} \right] q_1^*(t) + k_{12} q_2^*(t) & q_1^*(0) &= D^* \\ \dot{q}_2^*(t) &= - [k_{02} + x_d(t) + k_{12}] q_2^*(t) + k_{21} q_1^*(t) & q_2^*(0) &= 0 \\ \text{EGP}(t) &= \begin{cases} \text{EGP}_b - k_p [q_1(t) - q_{1b}] - x_p(t) q_1(t) & \text{if } \text{EGP}(t) > 0 \\ 0 & \text{otherwise} \end{cases} & & (A4) \\ \dot{x}_d(t) &= - k_a x_d(t) + k_{bd} [i(t) - ib] & x_d(0) &= 0 \\ \dot{x}_p(t) &= - k_a x_p(t) + k_{bp} [i(t) - ib] & x_p(0) &= 0 \\ g(t) &= \frac{q_1(t)}{V_1} \\ g^*(t) &= \frac{q_1^*(t)}{V_1} \end{aligned}$$

Table A1. Two-compartment model parameters

Parameter	Units	Value
<i>Glucose subsystem</i>		
V_1	dl/kg	1.58
V_T	dl/kg	2.63
k_{21}	min ⁻¹	0.043
k_{12}	min ⁻¹	0.059
k_{02}	min ⁻¹	0.006
k_d	min ⁻¹	0.0049
k_p	min ⁻¹	0.0044
$R_{d,0}$	mg · kg ⁻¹ · min ⁻¹	1.0
g_b	mg/dl	90
D	mg/kg	330
D^*	dpm/kg	1,500,000
<i>Insulin subsystem</i>		
k_a	min ⁻¹	0.045
k_{bd}	× 10 ⁻⁵ min ⁻² · μU · ml ⁻¹	3.76
k_{bp}	× 10 ⁻⁶ min ⁻² · μU · ml ⁻¹	6.49
i_b	μU/ml	7

See glossary for explanation of parameters.

where $q_i(t)$ and $q_i^*(t)$ ($i = 1, 2$) are, respectively, the cold and hot glucose masses in the i th compartment of the model.

The values of the model parameters are reported in Table A1. The values of V_1 , k_{21} , k_{12} , and k_{02} were taken from Ref. 21; $R_{d,0}$ was chosen to be equal to the value experimentally determined in Ref. 12; k_d was determined from Eq. A3; k_p was calculated with the assumption that glucose effectiveness on EGP is one-third of overall glucose effectiveness (11); parameter k_a was taken from Ref. 14; parameters k_{bd} and k_{bp} were chosen in such a way that the two-compartment model values of insulin sensitivity related to $R_d + \text{EGP}$ and to R_d only were equal to the analogous clamp-based values reported by Saad et al. (32) in normal subjects.

APPENDIX B: MONTE CARLO SIMULATION OF A HOT IVGTT

To obtain minimal model indexes that could be compared with the corresponding indexes of the two-compartment model, we resorted to Monte Carlo simulation. The two-compartment model equations were used to generate noise-

free cold and hot glucose data during a hot IVGTT. The mean insulin profile of either a standard or an insulin-modified IVGTT was used as input to the model (Fig. B1). It is of interest that the profiles of EGP generated in both occasions always assumed positive values, implying that it was not necessary to force EGP to be nonnegative. Subsequently, 200 realizations of noisy cold and hot glucose data were obtained by adding measurement noise of appropriate statistical characteristics to the noise-free data. Specifically, for cold (g , mg/dl) and hot (g^* , dpm/ml) glucose concentration, measurement noise was assumed to be independent, gaussian, and with a zero mean and standard deviations of 0.02 g and $30+0.018 g^*$, respectively. Each noisy data set was analyzed with the cold and hot minimal models. The cold minimal model was identified from cold glucose and insulin data and the hot minimal model from hot glucose and insulin data via nonlinear weighted least squares (13), with weights chosen optimally, i.e., equal to the inverse of the variance of the measurement error. As is usually done in practice, to mitigate the error of the single-compartment assumption, cold and hot glucose data up to 10 min after the glucose bolus were ignored in model identification. For the cold model, the value of g_b was chosen to be equal to the mean of the last two glucose data (at 210 and 240 min). Each

noisy data set yielded an estimate of fractional indexes S_G , S_I , S_G^* , and S_I^* , and volumes V and V^* . Results for the standard and insulin-modified IVGTT have been reported in Table 1.

APPENDIX C: TWO-COMPARTMENT MODEL INDEXES OF GLUCOSE EFFECTIVENESS AND INSULIN SENSITIVITY

Here we outline how indexes of cold and hot glucose effectiveness and insulin sensitivity can be derived from the parameters of the two-compartment model. For the sake of clarity, we first provide their definitions.

Cold glucose effectiveness is defined as the ability of glucose to promote its own disappearance by stimulating R_d and inhibiting EGP. It can be expressed mathematically as the derivative of $R_d + EGP$ with respect to glucose concentration at basal steady state

$$\text{Cold glucose effectiveness} \triangleq \left. \frac{\delta[R_d(t) + EGP(t)]}{\delta g(t)} \right|_{ss} \quad (C1)$$

Hot glucose effectiveness measures glucose effect on R_d only and is defined as

$$\text{Hot glucose effectiveness} \triangleq \left. \frac{\delta R_d(t)}{\delta g(t)} \right|_{ss} \quad (C2)$$

Insulin sensitivity is defined as the ability of insulin to enhance glucose effectiveness. Whereas cold insulin sensitivity measures insulin effect on both R_d and EGP, hot insulin sensitivity refers to R_d only

$$\text{Cold insulin sensitivity} \triangleq \left. \frac{\delta^2[R_d(t) + EGP(t)]}{\delta g(t)\delta i(t)} \right|_{ss} \quad (C3)$$

$$\text{Hot insulin sensitivity} \triangleq \left. \frac{\delta^2 R_d(t)}{\delta g(t)\delta i(t)} \right|_{ss} \quad (C4)$$

Plasma clearance rate is the ratio between R_d and plasma glucose concentration at steady state

$$\text{Plasma clearance rate} \triangleq \left. \frac{R_d(t)}{g(t)} \right|_{ss} \quad (C5)$$

Applying the above definitions to the two-compartment model described in APPENDIX A, one obtains indexes measuring cold and hot glucose effectiveness and insulin sensitivity and basal plasma clearance rate (GE , GE^* , IS , IS^* , and PCR). Details on the formal derivation of the indexes can be found in Vicini et al. (37). The expressions of the two-compartment model indexes are reported in Table C1.

In comparing the minimal model indexes obtained from the Monte Carlo simulation (Table 1) with the corresponding indexes of the two-compartment model, one is faced with the problem that the units are different. For instance, S_G is expressed in min^{-1} , whereas the two-compartment model glucose effectiveness, GE , is expressed in milligrams per kilogram per minute. As a matter of fact, the minimal model indexes S_G , S_I , S_G^* , and S_I^* are all fractional indexes, i.e., they refer to a unit of glucose distribution volume. As shown in Ref. 37, to convert the minimal model indexes to the same units of the two-compartment model indexes, the cold and hot indexes must be multiplied by the cold and hot minimal model volumes V and V^* , respectively. The expressions of the minimal model indexes multiplied by the respective volumes are reported in Table C1. It is worth mentioning that, for the

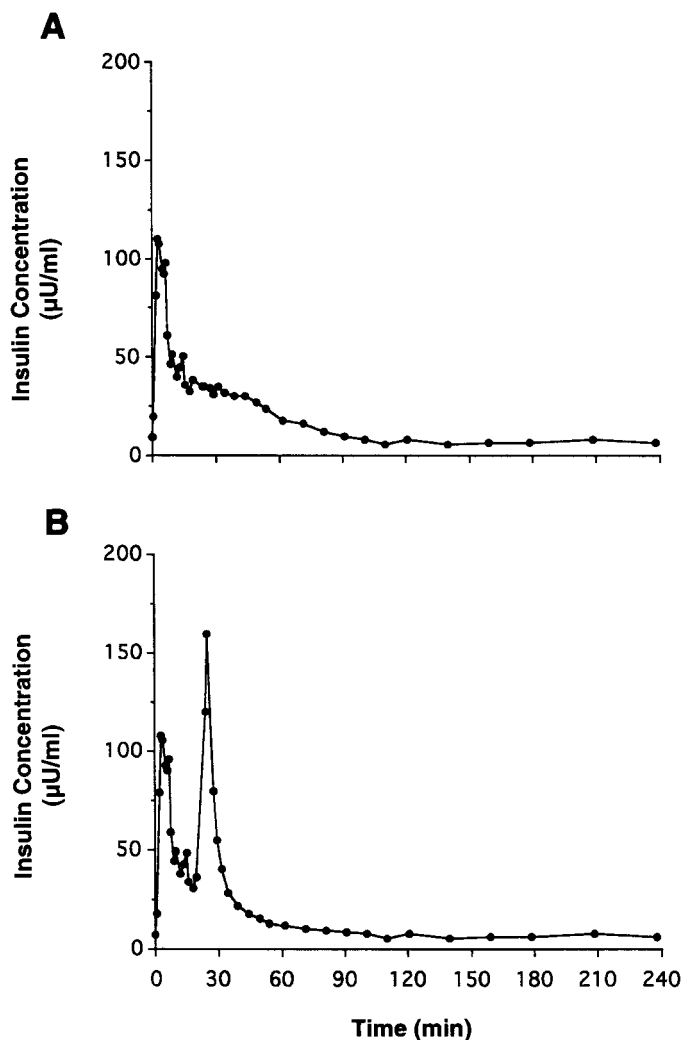


Fig. B1. Insulin profiles used in Monte Carlo simulation to assess the effect of insulin dynamics during the IVGTT on cold and hot minimal model indexes. Insulin profiles *A* and *B* are typical of a standard and an insulin-modified hot IVGTT, respectively.

Table C1. Glucose effectiveness, insulin sensitivity, and basal plasma clearance rate for two-compartment model, minimal models, and glucose clamp technique

	Two-Compartment Model	Minimal Models	Glucose Clamp
Cold glucose effectiveness, $\text{ml} \cdot \text{kg}^{-1} \cdot \text{min}^{-1}$	$\text{GE} = V_1 \left(k_d + k_p + \frac{k_{21}k_{02}}{k_{02} + k_{12}} \right)$	S_G	$S_{G,d(\text{clamp})} = \frac{\Delta \text{GINF}}{\Delta g} \Big _{i=b}$
Hot glucose effectiveness, $\text{ml} \cdot \text{kg}^{-1} \cdot \text{min}^{-1}$	$\text{GE}^* = V_1 \left(k_d + \frac{k_{21}k_{02}}{k_{02} + k_{12}} \right)$	$S_G^* V^*$	$S_{G(\text{clamp})} = \frac{\Delta R_d}{\Delta g} \Big _{i=b} \uparrow$
Cold insulin sensitivity, $\text{ml} \cdot \text{kg}^{-1} \cdot \text{min}^{-1} \cdot \mu\text{U}^{-1} \cdot \text{ml}$	$\text{IS} = V_1 \left(\frac{k_{bp}}{k_a} + \frac{k_{bd}}{k_a} \left[\frac{k_{21}k_{12}}{(k_{02} + k_{12})^2} \right] \right)$	S_{IV}	$S_{I(\text{clamp})} = \frac{\Delta \text{GINF}}{g \Delta i} \Big _{g=g_b}$
Hot insulin sensitivity, $\text{ml} \cdot \text{kg}^{-1} \cdot \text{min}^{-1} \cdot \mu\text{U}^{-1} \cdot \text{ml}$	$\text{IS}^* = V_1 \left(\frac{k_{bd}}{k_a} \left[\frac{k_{21}k_{12}}{(k_{02} + k_{12})^2} \right] \right)$	S_{IV}^*	$S_{I,d(\text{clamp})} = \frac{\Delta R_d}{g \Delta i} \Big _{g=g_b}$
Basal plasma clearance rate, $\text{ml} \cdot \text{kg}^{-1} \cdot \text{min}^{-1}$	$\text{PCR}_b = V_1 \left(k_d + \frac{R_{d,0}}{V_1 g_b} + \frac{k_{21}k_{02}}{k_{02} + k_{12}} \right)$	$S_G^* V^*$	$\text{PCR}_b = \frac{R_d}{g} \Big _{g=g_b}$

†In steady state, $R_d = (g/g^*)\text{INF}^*$, where INF^* is tracer infusion rate.

two-compartment model, glucose effectiveness and basal plasma clearance rate are different because R_d is not proportional to g , thus determining the presence of the nonzero intercept $R_{d,0}$. In contrast, because the hot minimal model assumes that R_d is proportional to g , one has $R_{d,0} = 0$, and glucose effectiveness and clearance rate coincide.

Cold and hot glucose effectiveness and insulin sensitivity can also be assessed under steady-state conditions by use of the glucose clamp technique (7, 11). Glucose effectiveness is measured from hyperglycemic clamps at basal insulin, whereas insulin sensitivity is measured from hyperinsulinemic, euglycemic clamps. The clamp-based indexes are thus derived on the basis of finite (Δ), rather than differential (δ), increments of glucose and insulin. Their expressions are reported in Table C1. As one can see, although the cold indexes reflect changes in the glucose infusion rate, GINF, and thus in both R_d and EGP, the hot indexes reflect changes in R_d only.

APPENDIX D: TWO-COMPARTMENT MODEL SIMULATION OF AN IVGTT AT BASAL INSULIN

The purpose here is to use the two-compartment model to describe the time courses of cold and hot glucose during a hot IVGTT in which insulin is maintained at the basal level.

Cold Glucose Decay

When insulin remains at the basal level throughout the IVGTT, insulin action is identically null and the two-compartment model equations for cold glucose become

$$\begin{aligned}
 \dot{q}_1(t) &= - \left[k_d + \frac{R_{d,0}}{q_1(t)} + k_{21} \right] q_1(t) + k_{12} q_2(t) + \text{EGP}_b - k_p [q_1(t) - q_{1b}] & q_1(0) &= D + q_{1b} \\
 \dot{q}_2(t) &= - [k_{02} + k_{12}] q_2(t) + k_{21} q_1(t) & q_2(0) &= q_{1b} [k_{21} / (k_{02} + k_{12})] \\
 g(t) &= \frac{q_1(t)}{V_1}
 \end{aligned} \tag{D1}$$

In the basal steady state, EGP equals R_d and thus

$$\text{EGP}_b = R_{db} = \text{PCR}_b g_b = V_1 \left[k_p + \frac{R_{d,0}}{V_1 g_b} + \frac{k_{21}k_{02}}{(k_{02} + k_{12})} \right] g_b \tag{D2}$$

Substitution of EGP_b given by Eq. D2 into Eq. D1 permits elimination of the term containing $R_{d,0}$. Using the position $\Delta q_i(t) = q_i(t) - q_{ib}$ for $i = 1, 2$, one obtains

$$\begin{aligned}
 \Delta \dot{q}_1(t) &= - [k_d + k_p + k_{21}] \Delta q_1(t) + k_{12} \Delta q_2(t) + D \delta(t) & \Delta q_1(0) &= 0 \\
 \Delta \dot{q}_2(t) &= - [k_{02} + k_{12}] \Delta q_2(t) + k_{21} \Delta q_1(t) & \Delta q_2(0) &= 0 \\
 \Delta g(t) &= \frac{\Delta q_1(t)}{V_1}
 \end{aligned} \tag{D3}$$

where $\delta(t)$ is the Dirac impulse function. Equation D3 indicates that, during an IVGTT at basal insulin, glucose decay above the baseline is the impulse response of a linear, second-order system with constant parameters. As a result, glucose decay is two-exponential

$$\Delta g(t) = D(A_1 e^{-\lambda_1 t} + A_2 e^{-\lambda_2 t}) \tag{D4}$$

where λ_1 and λ_2 are the fast and slow eigenvalues, respectively. Of note is that A_1 , A_2 , λ_1 , and λ_2 reflect the ability of glucose not only to promote R_d but also to inhibit EGP. Their values, reported in Table D1, have been derived from the two-compartment model parameters (Table A1) by calculat-

ing the transfer function of the system described by Eq. D3 and equating it to the Laplace transform of the two-exponential decay of Eq. D4 (13).

The fractional decay rate of incremental glucose concentration, k_G , which measures the fraction of glucose concentra-

above basal that declines per unit time, is given by

$$k_G(t) = -\frac{\Delta\dot{g}(t)}{\Delta g(t)} = \frac{(A_1\lambda_1 e^{-\lambda_1 t} + A_2\lambda_2 e^{-\lambda_2 t})}{(A_1 e^{-\lambda_1 t} + A_2 e^{-\lambda_2 t})} \quad (D5)$$

Hot Glucose Decay

During a hot IVGTT at basal insulin, the two-compartment model equations for hot glucose become

$$\begin{aligned} \dot{q}_1^*(t) &= -\left[k_d + \frac{R_{d,0}}{q_1(t)} + k_{21}\right]q_1^*(t) + k_{12}q_2^*(t) + D^*\delta(t) \\ q_1^*(0) &= 0 \\ \dot{q}_2^*(t) &= -[k_{02} + k_{12}]q_2^*(t) + k_{21}q_1^*(t) \\ q_2^*(0) &= 0 \end{aligned} \quad (D6)$$

$$g^*(t) = \frac{q_1^*(t)}{V_1}$$

If $R_{d,0}$ were equal to zero, the system described by Eq. D6 would be linear, and the decay of hot glucose concentration after the (cold + hot) glucose injection would coincide with the two-exponential impulse response of glucose kinetics in the basal steady state

$$g^*(t) = D^*(A_1^* e^{-\lambda_1^* t} + A_2^* e^{-\lambda_2^* t}) \quad (D7)$$

where λ_1^* and λ_2^* are the fast and slow eigenvalues of glucose kinetics in the basal state. Of note is that parameters A_1^* , A_2^* , λ_1^* , and λ_2^* reflect R_d only. Their values, reported in Table D1, have been derived from the two-compartment model parameters by calculating the transfer function of the linear system described by Eqs. D6 with $R_{d,0} = 0$ and equating it to the Laplace transform of the two-exponential decay of Eq. D7(13).

However, because $R_{d,0}$ is greater than zero, hot glucose decay is not two-exponential

$$g^*(t) = D^*(A_1^* e^{-\lambda_1^* t} + A_2^* e^{-\lambda_2^* t}) + \alpha(t) \quad (D8)$$

where the term $\alpha(t)$ is the deviation of the true hot glucose decay from the two-exponential function of Eq. D7. The fractional decay rate of hot glucose during the IVGTT at basal insulin, $k_G^*(t)$, is the ratio $\dot{g}(t)/g(t)$. The time course of $k_G^*(t)$ has been shown in Fig. 8.

APPENDIX E: $S_{G(\text{CLAMP})}$ FROM THE PARAMETERS OF THE TWO-COMPARTMENT MODEL

Here we show that the clamp-based measure of glucose effectiveness, $S_{G(\text{clamp})}$, can be expressed as a function of the

Table D1. Parameters of cold and hot glucose decay during a hot IVGTT at basal insulin

Parameter	Units	Value
<i>Cold glucose</i>		
A_1	kg/ml	0.0028
A_2	kg/ml	0.0036
λ_1	min ⁻¹	0.1094
λ_2	min ⁻¹	0.0079
<i>Hot glucose</i>		
A_1^*	kg/ml	0.0029
A_2^*	kg/ml	0.0035
λ_1^*	min ⁻¹	0.1106
λ_2^*	min ⁻¹	0.0093

See glossary for explanation of parameters.

parameters of the two-compartment model and is related to the area under the glucose decay curve during an IVGTT at basal insulin.

$S_{G(\text{clamp})}$ and the Two-Compartment Model

$S_{G(\text{clamp})}$ is measured from hyperglycemic clamp studies in which glucose concentration is elevated via an exogenous glucose infusion rate, and insulin concentration is maintained at the basal level (11). By applying the formal definition of glucose effectiveness reported in Eq. C1 to a hyperglycemic clamp at basal insulin, one finds that $S_{G(\text{clamp})}$ corresponds to the slope of the steady-state relationship between the exogenous glucose infusion rate, GINF, and plasma glucose concentration

$$S_{G(\text{clamp})} = \frac{\Delta(R_d - \text{EGP})}{\Delta g} \Big|_{i=i_b} = \frac{\Delta \text{GINF}}{\Delta g} \Big|_{i=i_b} \quad (E1)$$

To express $S_{G(\text{clamp})}$ as a function of the parameters of the two-compartment model, one must write the two-compartment model equations describing glucose dynamics during a hyperglycemic glucose clamp at basal insulin. They are the same as those derived in APPENDIX D for an IVGTT at basal insulin except that the exogenous glucose input is a variable glucose infusion, $\text{GINF}(t)$, instead of a bolus injection

$$\begin{aligned} \Delta\dot{q}_1(t) &= -[k_d + k_p + k_{21}]\Delta q_1(t) + k_{12}\Delta q_2(t) + \text{GINF}(t) \\ \Delta q_1(0) &= 0 \\ \Delta\dot{q}_2(t) &= -[k_{02} + k_{12}]\Delta q_2(t) + k_{21}\Delta q_1(t) \\ \Delta q_2(0) &= 0 \end{aligned} \quad (E2)$$

$$\Delta g(t) = \frac{\Delta q_1(t)}{V_1}$$

When an elevated steady state for glucose is achieved, the derivatives of Δq_1 and Δq_2 become null, and Eq. E2 yields the following relationship between ΔGINF and Δg

$$\Delta \text{GINF} = \Delta g V_1 \left[k_d + k_p + \frac{k_{21}k_{02}}{(k_{02} + k_{12})} \right] \quad (E3)$$

By substituting Eq. E3 into Eq. E1, one obtains

$$S_{G(\text{clamp})} = V_1 \left[k_d + k_p + \frac{k_{21}k_{02}}{(k_{02} + k_{12})} \right] \quad (E4)$$

It is of interest that the expression of $S_{G(\text{clamp})}$ in Eq. E4 is identical to the index of cold glucose effectiveness, GE, of the two-compartment model (see Table C1).

$S_{G(\text{clamp})}$ and the IVGTT at Basal Insulin

$S_{G(\text{clamp})}$ can also be expressed as a function of the impulse response parameters A_1 , A_2 , λ_1 , and λ_2 , which describe glucose decay during an IVGTT at basal insulin. To do so one has to integrate from zero to infinity Eq. D3, which describes the glucose glucose system during an IVGTT at basal insulin

$$\text{AUC}[\Delta g(t)] = \frac{D}{V_1 \left[k_d + k_p + \frac{k_{21}k_{02}}{(k_{02} + k_{12})} \right]} \quad (E5)$$

Because $\Delta g(t)$ is a two-exponential impulse response, $\text{AUC}[\Delta g(t)]$ can also be expressed as a function of the impulse

response parameters $A_1, A_2, \lambda_1,$ and λ_2

$$\text{AUC}[\Delta g(t)] = \frac{D}{\left(\frac{A_1}{\lambda_1} + \frac{A_2}{\lambda_2}\right)} \quad (E6)$$

By equating *Eqs. E5* and *E6* and remembering that the denominator of *Eq. E5* is equal to $S_{G(\text{clamp})}$ (see *Eq. E4*), one obtains

$$S_{G(\text{clamp})} = \frac{D}{\text{AUC}[\Delta g(t)]} = \frac{1}{\left(\frac{A_1}{\lambda_1} + \frac{A_2}{\lambda_2}\right)} \quad (E7)$$

APPENDIX F: INSULIN ACTION AND INSULIN SENSITIVITY OF THE MINIMAL MODELS

The purpose of this appendix is to investigate the relationships between insulin action and sensitivity of the two-compartment model and the minimal models.

In the two-compartment model, $x_d(t)$ is insulin action on glucose disposal, and $x_p(t)$ is insulin action on glucose production. The overall insulin action of the two-compartment model is thus $X(t) = x_p(t) + x_d(t)$. The insulin action of the cold minimal model, $x(t)$, differs from $X(t)$ for two reasons: the different model order (1 vs. 2 compartments) and the compartment where insulin action takes place (accessible vs. nonaccessible). To single out the effect of the monocompartmental approximation on $x(t)$, an “accessible-pool equivalent” profile of insulin action, denoted as $\tilde{X}(t)$, has been derived. $\tilde{X}(t) = x_p(t) + \tilde{x}_d(t)$, where $\tilde{x}_d(t)$ is the profile of insulin action on glucose uptake that, placed in the accessible pool of the two-compartment model, produces the same effect as $x_d(t)$ on plasma glucose concentration. Application of this definition to the two-compartment model (*Eq. A4*) leads to the following expression for $\tilde{x}_d(t)$

$$\tilde{x}_d(t) = k_{12} \frac{[\tilde{q}_2(t) - q_2(t)]}{q_1(t)} \quad (F1)$$

where $\tilde{q}_2(t)$ is glucose mass in the second compartment when the insulin-dependent glucose removal is moved to the accessible pool. Calculation of $\tilde{q}_2(t)$ requires solution of the mass-balance equation of the nonaccessible glucose pool (second equation in *A4*) without the insulin-dependent term

$$\begin{aligned} \dot{\tilde{q}}_2(t) &= -[k_{02} + k_{12}]\tilde{q}_2(t) + k_{21}q_1(t); \\ \tilde{q}_2(0) &= q_{1b}[k_{21}/(k_{02} + k_{12})] \end{aligned} \quad (F2)$$

Eq. F1 shows that $\tilde{x}_d(t)$ is such that the increase in the flux irreversibly leaving the accessible compartment, $\tilde{x}_d(t)q_1(t)$, exactly compensates the increase in the flux coming from the nonaccessible compartment. As a result, the time course of glucose concentration in the accessible pool remains unchanged.

The difference $\Delta_x(t) = \tilde{X}(t) - x(t)$ is the bias affecting the minimal model insulin action due to monocompartmental undermodeling. $\Delta_x(t)$ can be given an analytic expression by assuming that the minimal model is able to perfectly describe the glucose decay generated by the two-compartment model. In this case, $\Delta_x(t)$ can be derived by equating the expressions of the glucose fractional decay rate yielded by the two models. The fractional decay rate of glucose concentration of the minimal model is made up of two components, one depending

on insulin action and the other on glucose effectiveness (18)

$$\frac{\dot{g}(t)}{g(t)} = \frac{d \ln[g(t)]}{dt} - \left[x(t) + S_G \frac{\Delta g(t)}{g(t)} \right] \quad (F3)$$

The fractional decay rate of the two-compartment model can be calculated from *Eq. A1*

$$\frac{\dot{g}(t)}{g(t)} = \frac{d \ln[g(t)]}{dt} = - \left[\tilde{X}(t) + \frac{GE}{V_1} \frac{\Delta g(t)}{g(t)} + \frac{\gamma}{(k_{22})^2} \frac{\dot{\tilde{g}}_2(t)}{g(t)} \right] \quad (F4)$$

where $\gamma = k_{21}k_{12}$, $k_{22} = (k_{02} + k_{12})$, and $\tilde{g}_2(t)$ is glucose concentration in the second nonaccessible pool. Its structure is similar to the one of the minimal model except for an additional term proportional to the ratio between the derivative of glucose concentration in the nonaccessible pool and glucose concentration in the accessible pool. By equating *Eqs. F3* and *F4* one obtains an expression for $\Delta_x(t)$

$$\Delta_x(t) = \tilde{X}(t) - x(t) = - \left[\left(\frac{GE}{V_1} - S_G \right) \frac{\Delta g(t)}{g(t)} + \frac{\gamma}{(k_{22})^2} \frac{\dot{\tilde{g}}_2(t)}{g(t)} \right] \quad (F5)$$

Equation F5 shows that the bias affecting the minimal model insulin action has two components: the first is proportional to the minimal model underestimation of fractional glucose effectiveness, whereas the second is modulated by the rate of change of glucose concentration in the nonaccessible pool, normalized to glucose concentration in the accessible pool.

The bias affecting $x(t)$ influences the accuracy of S_I . In Ref. 18 we have shown that S_I is proportional to the integral of insulin action

$$S_I = \frac{\int_0^\infty x(t) dt}{\int_0^\infty [i(t) - i_b]} \quad (F6)$$

The fractional insulin sensitivity of the two-compartment model, IS/V_1 , is well approximated by the integral of $\tilde{X}(t)$ normalized to the area under the insulin concentration curve (6.46 vs. 6.52 $\text{min}^{-1} \cdot \mu\text{mol}^{-1} \cdot \text{ml}$). The agreement is not perfect because $\tilde{X}(t)$, being the accessible-pool equivalent of the two-compartment model insulin action, does not satisfy, like the minimal model insulin action $x(t)$ (*Eq. I*), the equation of a remote insulin compartment. The difference between the two-compartment and the cold minimal model estimates of insulin sensitivity is thus well approximated by

$$\Delta_{S_I}^* = \frac{IS}{V_1} - S_I \approx \frac{\text{AUC}[\Delta_x(t)]}{\text{AUC}[i(t) - i_b]} \quad (F7)$$

Analogous expressions for the difference between the two-compartment and the hot minimal model insulin action and insulin sensitivity can be derived by following an approach similar to that just outlined for the cold model. Δ_x^* , which is the difference between the two-compartment insulin action on R_d (applied to the accessible pool) and the hot minimal model insulin action, is given by

$$\begin{aligned} \Delta_x^*(t) &= \tilde{x}_d^*(t) - x^*(t) \\ &= - \left[\left(\frac{GE^*}{V_1} - S_G^* \right) + \frac{\gamma}{(k_{22})^2} \frac{\dot{\tilde{g}}_2^*(t)}{g^*(t)} + \frac{R_{d,0}}{V_1 g(t)} \right] \end{aligned} \quad (F8)$$

where $\bar{x}_d^*(t)$ is the "accessible-pool equivalent" profile of two-compartment insulin action on glucose disposal calculated from tracer data. $\bar{x}_d^*(t)$ is calculated from the two-compartment model (Eq. A1) so as to produce the same effect on hot glucose concentration as $x_d(t)$; GE^*/V_1 is fractional hot glucose effectiveness of the two-compartment model; $\bar{g}_2^*(t)$ is hot glucose concentration in the nonaccessible glucose pool when insulin-dependent glucose removal takes place in the accessible pool. The expression of $\Delta_x^*(t)$ is similar to that of $\Delta_x(t)$ but includes an additional term proportional to $R_{d,0}$ that accounts for the fact that the hot minimal model does not describe the inhibitory effect of glucose on its own clearance. $\Delta_{S_I^*}$, i.e., the difference between the (fractional) insulin sensitivity on R_d of the two-compartment model and S_I^* , can be calculated as previously done for S_I

$$\Delta_{S_I^*} = \frac{IS^*}{V_1} - S_I^* \approx \frac{AUC[\Delta_x^*(t)]}{AUC[\bar{i}(t) - i_b]} \quad (F9)$$

where the hot fractional insulin sensitivity of the two-compartment model, IS^*/V_1 , is well approximated by the integral of $\bar{x}_d^*(t)$ normalized to the area under the insulin concentration curve (5.02 vs. 5.78 $\text{min}^{-1} \cdot \mu\text{mol}^{-1} \cdot \text{ml}$). The agreement is not perfect because $\bar{x}_d^*(t)$, the tracer-based accessible-pool equivalent of the two-compartment model insulin action on glucose disposal, does not satisfy, as the minimal model insulin action $x^*(t)$ (Eq. 2), the equation of a remote insulin compartment.

Address for correspondence and reprint requests: C. Cobelli, Dept. of Electronics and Informatics, Univ. of Padova, 35131 Padova, Italy. (E-mail: cobelli@dei.unipd.it).

Received 26 March 1996; accepted in final form 19 February 1999.

REFERENCES

- Ader, M., G. Pacini, Y. J. Yang, and R. N. Bergman. Importance of glucose per se to intravenous tolerance. Comparison of the minimal-model prediction with direct measurement. *Diabetes* 34: 1092–1103, 1985.
- Avogaro, A., J. D. Bristow, D. M. Bier, C. Cobelli, and G. Toffolo. Stable-label intravenous glucose tolerance test minimal model. *Diabetes* 38: 1048–1055, 1989.
- Avogaro, A., P. Vicini, A. Valerio, A. Caumo, and C. Cobelli. The hot but not the cold minimal model allows precise assessment of insulin sensitivity in NIDDM subjects. *Am. J. Physiol.* 270 (Endocrinol. Metab. 33): E532–E540, 1996.
- Basu, A., A. Caumo, F. Bettini, A. Gelisio, A. Alzaid, C. Cobelli, and R. A. Rizza. Impaired basal glucose effectiveness in NIDDM. Contribution of defects in glucose disappearance and production, measured using an optimized minimal model independent protocol. *Diabetes* 46: 421–432, 1997.
- Beard, J. C., R. N. Bergman, W. K. Ward, and D. Porte. The insulin sensitivity index in nondiabetic man: correlation between clamp-derived and IVGTT-derived values. *Diabetes* 35: 362–369, 1986.
- Bergman, R. N. Toward physiological understanding of glucose tolerance: minimal-model approach. *Diabetes* 38: 1512–1527, 1989.
- Bergman, R. N., D. T. Finegood, and M. Ader. Assessment of insulin sensitivity in vivo. *Endocr. Rev.* 6: 45–86, 1985.
- Bergman, R. N., Y. Z. Ider, C. R. Bowden, and C. Cobelli. Quantitative estimation of insulin sensitivity. *Am. J. Physiol.* 236 (Endocrinol. Metab. Gastrointest. Physiol. 5): E667–E677, 1979.
- Bergman, R. N., N. L. S. Phillips, and C. Cobelli. Physiologic evaluation of factors controlling glucose tolerance in man. Measurement of insulin sensitivity and beta-cell sensitivity from the response to intravenous glucose. *J. Clin. Invest.* 68: 1456–1467, 1981.
- Bergman, R. N., R. Prager, A. Volund, and J. M. Olefsky. Equivalence of the insulin sensitivity index in man derived by the minimal model and the euglycemic glucose clamp. *J. Clin. Invest.* 79: 790–800, 1987.
- Best, J. D., S. E. Kahn, M. Ader, R. M. Watanabe, T.-C. Ni, and R. N. Bergman. Role of glucose effectiveness in the determination of glucose tolerance. *Diabetes Care* 19: 1018–1030, 1996.
- Best, J. D., J. Taborsky, Jr., J. B. Halter, and D. Porte, Jr. Glucose disposal is not proportional to plasma glucose level in man. *Diabetes* 30: 847–850, 1981.
- Carson, E. R., C. Cobelli, and L. Finkelstein. *The Mathematical Modelling of Metabolic and Endocrine Systems*. New York: Wiley, 1983.
- Caumo, A., and C. Cobelli. Hepatic glucose production during the labeled IVGTT: estimation by deconvolution with a new minimal model. *Am. J. Physiol.* 264 (Endocrinol. Metab. 27): E829–E841, 1993.
- Caumo, A., and C. Cobelli. Bayesian identification of a new two-compartment minimal model corrects S_G overestimation and S_I underestimation (Abstract). *Diabetologia* 41, Suppl. 1: A199, 1998.
- Caumo, A., C. Cobelli; D. T. Finegood. Minimal model estimate of glucose effectiveness: role of the minimal model volume and of the second hidden compartment. *Am. J. Physiol.* 274 (Endocrinol. Metab. 37): E573–E576, 1998.
- Caumo, A., A. Giacca, M. Morgese, G. Pozza, P. Micossi, and C. Cobelli. Minimal model of glucose disappearance: lessons from the labeled IVGTT. *Diab. Med.* 8: 822–832, 1991.
- Caumo, A., P. Vicini, and C. Cobelli. Is the minimal model too minimal? *Diabetologia* 39: 997–1000, 1996.
- Cobelli, C., G. Pacini, G. Toffolo, and L. Saccà. Estimation of insulin sensitivity and glucose clearance from minimal model: new insights from labeled IVGTT. *Am. J. Physiol.* 250 (Endocrinol. Metab. 13): E591–E598, 1986.
- Cobelli, C., and K. Thomaseth. The minimal model of glucose disappearance: optimal input studies. *Math. Biosci.* 83: 125–155, 1987.
- Cobelli, C., G. Toffolo, and E. Ferrannini. A model of glucose kinetics and their control by insulin, compartmental and noncompartmental approaches. *Math. Biosci.* 72: 291–315, 1984.
- Cobelli, C., P. Vicini, and A. Caumo. If the minimal model is too minimal, who suffers more: S_G or S_I ? *Diabetologia* 40: 362–363, 1997.
- Cobelli, C., P. Vicini, G. Toffolo, and A. Caumo. The hot IVGTT minimal models: simultaneous assessment of disposal indices and hepatic glucose release. In: *The Minimal Model Approach and Determinants of Glucose Tolerance*, edited by J. Lovejoy and R. N. Bergman. Baton Rouge, LA: Louisiana State University Press, 1997. (Pennington Nutrition Ser.)
- Finegood, D. T., and D. Tzur. Reduced glucose effectiveness associated with reduced insulin release: an artifact of the minimal-model method. *Am. J. Physiol.* 271 (Endocrinol. Metab. 34): E485–E495, 1996.
- Jacquez, J. A. Theory of production rate calculations in steady and non-steady states and its application to glucose metabolism. *Am. J. Physiol.* 262 (Endocrinol. Metab. 25): E779–E790, 1992.
- Katz, H., P. Butler, M. Homan, A. Zerman, A. Caumo, C. Cobelli, and R. Rizza. Hepatic and extrahepatic insulin action in humans: measurement in the absence of non-steady-state error. *Am. J. Physiol.* 264 (Endocrinol. Metab. 27): E561–E566, 1993.
- Mari, A. Assessment of insulin sensitivity with minimal model: role of model assumptions. *Am. J. Physiol.* 272 (Endocrinol. Metab. 35): E925–E934, 1997.
- Norwich, K. N. Molecular dynamics. In: *The Kinetics of Tracers in the Intact Organism*. Oxford, UK: Pergamon, 1977.
- Prigeon, R. L., M. E. Roder, S. E. Kahn, Jr., and D. Porte. The effect of insulin dose on the measurement of insulin sensitivity by the minimal model technique: evidence for saturable insulin transport in humans. *J. Clin. Invest.* 97: 501–507, 1996.
- Quon, M. J., C. Cochran, S. I. Taylor, and R. C. Eastman. Non-insulin mediated glucose disappearance in subjects with IDDM: discordance between experimental results and minimal model analysis. *Diabetes* 43: 890–896, 1994.

31. **Rostami-Hodjegan, A., S. R. Peacey, E. George, S. R. Heller, and G. T. Tucker.** Population-based modeling to demonstrate extrapancreatic effects of tolbutamide. *Am. J. Physiol.* 274 (*Endocrinol. Metab.* 37): E758–E771, 1998.
32. **Saad, M. F., R. L. Anderson, A. Laws, R. M. Watanabe, W. W. Kades, Y. D. Chen Ida, R. E. Sands, D. Pei, P. J. Savage, and R. N. Bergman for the IRAS.** A comparison between the minimal model and the glucose clamp in the assessment of insulin sensitivity across the spectrum of glucose tolerance. *Diabetes* 43: 1114–1121, 1994.
33. **Saad, M. F., G. M. Steil, W. W. Kades, M. F. Ayad, W. A. Elsewafy, R. Boyadjian, S. D. Jinagouda, and R. N. Bergman.** Differences between the tolbutamide-boosted and insulin-modified minimal model protocols. *Diabetes* 46: 1167–1171, 1997.
34. **Saad, M. F., G. M. Steil, M. Riad-Gabriel, A. Kahn, A. Sharma, R. Boyadjian, S. D. Jinagouda, and R. N. Bergman.** Method of insulin administration has no effect on insulin sensitivity estimates from the insulin-modified minimal model protocol. *Diabetes* 46: 2044–2048, 1997.
35. **Steil, G. M., K. Rebrin, S. D. Mittelman, and R. N. Bergman.** Role of portal insulin delivery in the disappearance of intravenous glucose and assessment of insulin sensitivity. *Diabetes* 47: 714–720, 1998.
36. **Verdonk, C. A., R. A. Rizza, J. E. Gerich.** Effects of plasma glucose concentration on glucose utilization and glucose clearance in normal man. *Diabetes* 30: 535–537, 1981.
37. **Vicini, P., A. Caumo, and C. Cobelli.** The hot IVGTT two-compartment minimal model: indexes of glucose effectiveness and insulin sensitivity. *Am. J. Physiol.* 273 (*Endocrinol. Metab.* 36): E1024–E1032, 1997.
38. **Vicini, P., A. Caumo, and C. Cobelli.** Glucose effectiveness and insulin sensitivity from the single compartment minimal models of glucose disappearance: consequences of undermodeling assessed by Monte Carlo simulation. *IEEE Trans. Biomed. Eng.* 46: 130–137, 1999.
39. **Vicini, P., J. J. Zachwieja, K. E. Yarasheski, D. M. Bier, A. Caumo, and C. Cobelli.** Glucose production during an IVGTT by deconvolution: validation with the tracer-to-tracee clamp technique. *Am. J. Physiol.* 276 (*Endocrinol. Metab.* 39): E285–E294, 1999.
40. **Yang, Y. J., J. H. Youn, and R. N. Bergman.** Modified protocols improve insulin sensitivity estimation using the minimal model. *Am. J. Physiol.* 253 (*Endocrinol. Metab.* 16): E595–E602, 1987.

